Faculty of Medicine
University of Szeged
Szeged, Hungary

Application of microarray and quantitative real-time PCR methods in oncology

Ph.D. Thesis

2006.

Liliána Z. Fehér

Biological Research Center

of the Hungar{an Academy of Sciences

Laboratory of Functional Genomics

CONTENT

I. PUBLICATIONS RELATED TO THE THESIS

[1] **Liliána Z. Fehér**, Margit Balázs, János Z. Kelmen, István Németh, Zoltán Varga-Orvos, László G. Puskás (2006) Improved DOP-PCR-based representational whole-genome amplification using quantitative real-time PCR. *Diagn. Mol. Pathol*. 15:43-8.

[2] Judit Nagy, **Liliána Z. Fehér**, István Sonkodi, József Lesznyák, Béla Iványi, László G. Puskás (2005) A second field metachronous Merkel cell carcinoma of the lip and the palatine tonsil confirmed by microarray-based comparative genomic hybridization. *Virchows Arch*. 446:278-86.

[3] Balázs Döme, Erzsébet Rásó, Judit Dobos, Livia Mészáros, Norbert Varga, László G. Puskás, **Liliána Z. Fehér,** Tamár Lőrincz, Andrea Ladányi, Mohit Trikha, Kenneth V. Honn, József Tímár (2005) Parallel expression of alphaIIbbeta3 and alphavbeta3 integrins in human melanoma cells upregulates bFGF expression and promotes their angiogenic phenotype. *Int. J. Cancer*. 116:27-35.

[4] Zsolt B. Nagy, János Z. Kelemen, **Liliána Z. Fehér**, Ágnes Zvara, Kata Juhász, László G. Puskás (2005) Real-time polymerase chain reaction-based exponential sample amplification for microarray gene expression profiling. *Anal. Biochem.* 337:76-83.

II. AIMS

[1] Development of an improved degenerate oligonucleotide-primed (DOP) PCR-based representational whole-genome amplification method using quantitative real-time PCR (QRT-PCR).

[2] Identification of an uncommon metastasis of Merkel cell carcinoma (MCC) cell carcinoma with the improved whole genome amplification and comparative genome hybridization (CGH) technique with DNA microarrays.

[3] Determining changes in chromosome copy numbers of papillary thyroid carcinomas (PTC) of good disease outcome and an aggressive type of PTC derived from the same patient using CGH-microarray and QRT-PCR techniques.

[4] Identification of gene markers based on copy number changes for classification PTCs of different disesase courses.

[5] Determining the angiogenic phenotype of αIIbβ3 integrin-transduced human melanoma cells expressing integrin αvβ3 using DNA-microarray technology to reveal the underlying pathomechanism.

III. ABBREVIATIONS

AKAP13:	A-kinase anchor protein 13
Arf6:	ADP-ribosylation factor 6
APTC:	An aggressive type of papillary thyroid carcinoma
ATC:	Anaplastic thyroid cancer
BAC:	Bacterial artificial chromosome
Bcl-2:	B-cell CLL/lymphoma 2
bFGF:	Basic fibroblast growth factor
BRAF:	v-raf murine sarcoma viral oncogene homolog B1
CGH:	Comparative genome hybridization
CHO:	Chinese hamster ovary
COX-2:	Prostaglandin-endoperoxide synthase 2
Dbl:	MCF.2 cell line derived transforming sequence
DGGE:	Denaturing gradient gel electrophoresis
DOP-PCR:	Degenerate oligonucleotide-primed PCR
EIF4EBP3:	Eukaryotic initiation factor 4E-binding protein 3
FGF7:	Fibroblast growth factor 7
FISH:	Fluorescent *in situ* hybridization
FTC:	Follicular thyroid carcinoma
GAP:	GTPase-activating protein
GEF:	Guanine nucleotide exchange factor
GPTC:	Papillary thyroid carcinoma of good disease outcome
HRAS:	v-Ha-ras Harvey rat sarcoma viral oncogene homolog
IRS-PCR:	Infrequent-restriction-site polymerase chain reaction
IPTC:	Intermediate papillary thyroid carcinoma
Ki-67:	Antigen identified by monoclonal antibody Ki-67
KRAS:	v-Ki-ras2 Kirsten rat sarcoma viral oncogene homolog
LA-PCR:	Linker adapter polymerase chain reaction
Lbc:	Lymphoid blast crisis oncogene
LMP:	Ligation mediated polymerase chain reaction
LOH:	Loss of heterozygosity
MAPK:	Mitogen-activated protein kinase
MAPKK:	Mitogen-activated protein kinase kinase
MCC:	Merkel cell carcinoma
MDA:	Multiple displacement amplification
NRAS:	Neuroblastoma RAS viral (v-ras) oncogene homolog
PAC:	P1-derived artificial chromosome
PEP:	Primer extension preamplification
PIK3CA:	Phosphatydilinositol 3-kinase, catalytic, alpha polypeptide
PI3K:	Phosphatidylinositol 3-kinase
PTC:	Papillary thyroid cancer
PTEN:	Phosphatase and tensin homolog
QRT-PCR:	Quantitative real-time PCR
RET:	REarranged during Transfection proto-oncogene
RT:	Reverse transcription
RT-PCR:	Reverse transcription-polymerase chain reaction
SDA:	Strand displacement amplification
SKY:	Spectral karyotyping
SNP:	Single-nucleotide polymorphism
SSCP:	Single-stranded confirmational polymorphism
TB10:	Thymosin beta 10
TLAD:	T7-based linear amplification
TNM:	Tumour, node, metastasis
TPO:	Thyroid peroxidase
Tre-2:	Ubiquitin specific peptidase 6
TSH:	Thyroid stimulating hormone
VEGF-C:	Vascular endothelial growth factor C
vWF:	von Willebrand factor

IV. ABSTRACT

The technological advances in molecular biology have proven invaluable to the understanding of the pathogenesis of human cancer. The application of molecular technology to the study of cancer has not only led to advances in tumour diagnosis, but has also provided markers for the assessment of prognosis and disease progression. The amount of genomic DNA from archived clinical samples available for genetic studies can often be limited. Diverse whole genome amplification methods are applied to provide a sufficient amount of DNA for CGH, single nucleotide polymorphism (SNP) and microsatellite analyses. CGH allows identification of changes in relative copy number of DNA sequences (gains and losses) and provides information on the primary genetic changes. Currently the microarray-based CGH serves as an excellent method of display. In this thesis an improved DOP-PCR technique, and its application in the case of two clinical studies are described. The effect of αIIbβ3 integrin transfection onto gene expression pattern of human melanoma cells was also analysed.

In genomic studies the reliability of the amplification techniques is particularly important. In PCR-based approaches, the plateau-effect can seriously alter the original relative copy number of certain chromosomal regions. To eliminate this distorting effect, we improved the standard DOP-PCR technique by following the amplification status with QRT-PCR. With real-time detection of the products, we managed to eliminate DNA over-amplification. Probes were generated from 10 different tumour samples by using non-amplified and amplified genomic DNA with DOP-PCR and DOP-PCR combined with QRT-PCR. To demonstrate the reliability of the QRT-PCR based amplification protocol, altogether 152 relative copy number changes of 44 regions were determined. There was a 85.6% concordance in copy number alterations between the QRT-PCR protocol and the non-amplified samples, while this value was only 63.8% for the traditional DOP-PCR. Our results demonstrate that this protocol preserves the original copy number of different chromosomal regions in amplified genomic DNA – more accurately than standard DOP-PCR techniques. This improved genomic amplification technique was also applied in two clinical cases.

In the first case, MCC was diagnosed in a 79-year-old Caucasian woman. This malignant, neuroendocrin tumour was localized to the upper lip. After successful cryosurgery and a 7-year tumour-free period, a new tumour developed in her palatine tonsil. The regional

lymph nodes were devoid of metastasis. After a long tumour-free period, an anaplastic carcinoma with neuroendocrine features developed in her palatine tonsil, raising the possibility of a late haematogenous metastasis, a second field tumour, or a second primary tumour. The genomic DNA obtained from the paraffin-embedded two tumours and unaffected lymphatic tissue was amplified with our improved DOP-PCR protocol for CGH and DNA microarray techniques to assess the genetic relationship of the tumours. The partly similar and partly different molecular patterns indicated a genetic relationship between the tumours, and excluded the possibility that the tonsillar tumour was a metastasis. Our results suggest that a genetically altered field was the reason for the development of the tonsillar cancer; thus, it can be pathogenetically regarded as a second field tumour.

The improved DOP-PCR technique was also employed for the detection of molecular patterns of PTC of different disease courses. PTC is the most common type of thyroid cancers, making up about 80% of all types. Unlike some other tumours, the generally excellent outcome for PTC is usually not affected by spread of the cancer to the lymph nodes. All the same in some cases it transforms into a dedifferentiated invasive tumour with an unfavourable outcome. Our aim was to identify gene copy number alteration as a marker or set of markers in order to predict individual patient outcome more effectively than existing staging methods; for this reason, we performed CGH-array analysis of primary- and terminal-stage APTCs, comparing them with PTC of good disease outcome (GPTC) obtained from paraffin-embedded tissue. On the basis of CGH-array and confirming QRT-PCR results, six regions were selected for further investigation of 34 PTCs of different disease courses. Two groups were constructed according to the disease groups: 'A' group: 10 cases of GPTCs; 'B' group: 14 cases of intermediate (IPTC) and 10 cases of APTCs (I/APTC). In the present study, Tre-2 oncogene was found to be over-represented in 80% of both the GPTC and the I/APTC groups. Thymosin beta 10 (TB10) was amplified in 62.5% of APTC, whereas in the case of the GPTC group, the ratio of DNA gains was only 20%. A similarly patterned difference, but with lower percentage rates, could be detected in our examined Image EST region, which is mapped to the AKAP13 gene. Two regions were under-represented in a different proportion: eukaryotic initiation factor 4E-binding protein 3 (EIF4EBP3) and KIAA0549 genes. The sixth examined gene, namely fibroblast growth factor 7 (FGF7), demonstrated both DNA gains and losses with a smaller rate.

Copy number changes of the above mentioned six loci alone are still not sufficient for classifying the tumours; however, on the basis of our results, the synchronous presence of the amplified TB10 and Image EST (Acc. No. R78712) regions could serve a good diagnostic – or possibly prognostic – marker for aggressive thyroid carcinoma.

In our other study we developed a cDNA amplification method within which – similarly to the whole genomic DNA amplification – the course of amplification was followed using QRT-PCR. With this approach low quantity RNA sample could also be reliably analysed, which is especially important in assessing gene expression pattern analysis for instance the molecular mechanisms in different tumours.

In cancerous tissues new vessels are required to provide cancer cells with nutrients and are targets for invading cancer cells themselves. The transfection of the platelet integrin αIIbβ3 into human melanoma cells expressing integrin αvβ3 promoted their *in vivo* (but not *in vitro*) growth and cell survival. To reveal the underlying pathomechanism, we have analysed the angiogenic phenotype of αIIbβ3 integrin-transduced human melanoma cells expressing integrin αvβ3. The cDNA microarray analysis of the 19H cells revealed 12 down-regulated and 36 up-regulated genes. Three out of nineteen known genes, up-regulated significantly in αIIbβ3-transfected 19H melanoma cells, are endothelial cell-specific genes: CD34, endothelin receptor B, and prostaglandin I-2 synthase. We propose that the illegitimate expression of αIIbβ3 integrin in human melanoma cells already expressing αvβ3 integrin may alter their *in vivo* growth properties due to the modulation of their angiogenic phenotype.

V. INTRODUCTION

5.1. Functional genomics in oncology

Dramatic technological advances have resulted in overwhelming information on biological systems. Advances in manipulating and sequencing DNA triggered the last such leap. More than twenty years ago this technology began finding its way into biology laboratories and multiple landmark discoveries have followed, including the sequencing of the genomes of several prokaryotic and eukaryotic species. This, in turn, spawned a new interest in bioinformatics, structural biology, and high-throughput methods that would allow scientists to look at the response of the entire genome to physiological, pharmacological, and pathological changes.

The development of our understanding of the cell and molecular biology of the neoplastic process has closely paralleled advances in our understanding of tumour cell and molecular biology of normal cells. The vast majority of the phenotypic and genotypic alterations seen in neoplasia—i.e., cells in the stage of progression—are a direct result of the primary characteristic of this stage, evolving karyotypic instability. The discoveries of chemical, physical, and biological carcinogenic agents and their actions have been among the most exciting and significant in our understanding of the causation of cancer and of many aspects of its prevention, but nothing has intrigued the biological scientist more than the molecular differences between cancer cells and normal cells.

Many researchers have described a number of processes and functions in the cell and in molecular biology of preneoplasia and neoplasia, namely the following: glycolysis, regulation of gene expression, signal transduction, transcription factors, cell cycle, DNA methylation, apoptosis, telomerase mechanism, unique or mutant protein expression, unique lipids and carbohydrates. However, it is important to note that there is no single component of any of these processes that is ubiquitously abnormal in all neoplasms. However, the majority of neoplasms exhibit at least one defective process in each of those listed. A comparison of the cellular and molecular biology of preneoplasia with that of neoplasia does, however, emphasize the importance of an understanding of the molecular transition between these two stages as critical to our understanding of the ultimate formation of the cancer cell.

For the identification of chromosomal abnormalities, high-throughput methods are becoming more and more routine and they are comprising of fluorescent *in situ* hybridization (FISH) (1, 2), spectral karyotyping (SKY) (3), CGH (4), and microsatellite analysis (5). FISH has a prominent role in the molecular analysis of cancer and can be used for the detection of numerical and structural chromosomal abnormalities. The recently described SKY, in which all human metaphase chromosomes are visualized in specific colors, allows for the definition of all chromosomal rearrangements and marker chromosomes in a tumour cell. Protocols for the detection of chromosomal rearrangements by PCR and RT-PCR are described, as well as the technique of DNA fingerprinting, a powerful tool for studying somatic genetic alterations in tumourigenesis. A number of approaches to identify mutations are detailed, and include single-stranded confirmational polymorphism (SSCP) (6), denaturing gradient gel electrophoresis (DGGE) (7), the nonisotopic RNase cleavage assay (8), the protein truncation assay (9), and DNA sequencing (10). A change in DNA methylation status is commonly observed in cancer, and specific methodology for methylation analysis (11) is also provided by this volume. A reduction in telomere length, together with expression of the telomere maintenance enzyme, telomerase, has been described in case of a wide range of human cancers (12). The research field of the spotted DNA microarray is dealing with the structure and activity of genomes and global relationships between genotype and phenotype. The birth of the field can be traced back to three seminal papers (13-15). Similar interminable approaches have been used to monitor relative protein levels (16), protein functions (17), cellular activities (18), and molecular interactions (19). The analysis of gene expression represents a key area of research in the study of human cancer. Global RNA expression analysis using microarray technology (20) allows the identification of genes that are differentially expressed in tumour versus normal tissues (21). This is a powerful approach for identifying genes that are central to disease development or progression and can also identify new prognostic markers.

In this thesis we describe a new QRT-PCR-based DOP-PCR method which is capable of preserving the original copy number of different chromosomal regions in amplified genomic DNA. Furthermore, genomic imbalances were detected by CGH with microarray to assess the genetic relationship between MCC and later appearing tonsillar tumour, in addition to molecular genetic markers in the case of PTCs of different disease courses. Finally, the

gene expression pattern of αIIbβ3 integrin transfected human melanoma cells was demonstrated to define molecular pathomechanism of increased melanoma growth and angiogenesis by DNA microarray technique.

5.2. Quantitative real-time PCR

5.2.1. Applications of QRT-PCR

The ability to monitor the real-time progress of the PCR completely revolutionizes the way one approaches PCR-based quantification of DNA and RNA. The development of fluorescent detection systems, capable of monitoring PCR product accumulation has greatly improved the reliability of QRT-PCR. Quantitative PCR is aimed to determine the absolute or relative amounts of RNA or DNA sequences in a given sample. There is a well-established inverse correlation between the template concentration and the duration of the lag phase of the PCR. An entire generation of automated systems has been developed to exploit this. Using any of several different chemistries, the accumulation of PCR product is monitored until a predetermined threshold is reached. This lag time is then compared with a standard curve and a concentration calculated (22). Reactions are characterized by the point in time during cycling when amplification of a PCR product is first detected rather than the amount of PCR product accumulated after a fixed number of cycles. The higher the starting copy number of the nucleic acid target, the sooner a significant increase in fluorescence is observed. Advantages of this method not only include the elimination of differences in reaction mix volumes and conditions that may occur in separate samples, but importantly it also allows reference of RNA or DNA quantitation to an internal control. Consequently, this system of quantitation has the advantage in that it allows the quantitation of multiple sequences from a single sample and a single experiment of amplification without the need of standardization for each sequence.

The QRT-PCR technology is now widely used, especially in such areas as therapeutic monitoring at the assessment of residual disease after treatment of leukemia and lymphoma (23-25), quality control, disease diagnosis (26), the detection of viral nucleic acids, regulation of gene expression (27), and the detection of gene amplification or deletion and of aneuploidy.

5.2.2. Determination of copy number changes in whole genome and validation of CGH-array profiles

PCR and QRT-PCR are now well-established methods for the study of nucleic acid sequences in histological material. QRT-PCR is the reliable detection and measurement of products generated during each cycle of the PCR which are directly in proportion to the amount of template prior to the start of the PCR process.

The applications of QRT-PCR are diverse and numerous, including such areas as DNA/cDNA copy number measurement in genomic or viral DNA/RNA, functional genomics including mRNA expression analysis, allelic discrimination assays and confirmation of microarray data. Upstream modifications to the technique, including the use of laser capture microdissection, add an extra dimension in facilitating the production of homogenous cell populations from complex tissue sections for more accurate quantitative analysis.

The challenge is to put the technology to full use by identification of the genetic changes that are important in human disease. Knowledge of these changes will permit the establishment of rapid, cost-effective tests for diagnosis and monitoring of disease as well as providing a basic understanding of their underlying causes. These developments will be enhanced by unravelling of the complete human genome and by improvements in techniques for gene amplification using histological samples.

Data obtained from the microarray experiments need validation by independent techniques like QRT-PCR or metaphase CGH. To determine the relative copy number ratios of the genome and in order to strengthen the CGH-array data, QRT-PCR was applied in this study.

5.3. Whole genome amplification techniques

High-throughput genomic analysis requires large amounts of template; however, the typical yield of DNA from individual samples can be often limited. The primary drawback of the use of laser capture microscopy in DNA analysis is that microdissections yield insufficient nucleic acids due to low genomic DNA recovered from small sample sizes. With samples such as these, the ability to conduct sample amplification becomes imperative, to ensure that enough material is available for genetic analysis. There are three basic techniques to amplify

the entire genomic DNA: PCR-based approaches (28-38), strand or multiple displacement amplification (SDA or MDA) (39) and T7-based linear amplification (TLAD) (40).

5.3.1. Strand or multiple displacement amplification (SDA or MDA) and T7-based linear amplification

The SDA and MDA isothermal methods employ the unique biochemical properties of Phi29 DNA polymerase to amplify linear DNA. These techniques are based on the rolling circle amplification by which circular DNA molecules such as plasmids or viruses frequently replicate. These rolling circle amplification methods were initially adapted for the amplification of large circular DNA templates (41, 42) and more recently for the amplification of genomic DNA (39). The drawback of SDA is that the efficiency of amplification depends on the length of the template. T7-based linear amplification is applicable for the amplification of genomic DNA of varying fragment size and quality, and it is based on a protocol devised by Phillips and Eberwine for the amplification of mRNA for cDNA microarrays (40, 43).

5.3.2. PCR-based genomic DNA amplification methods

The inter-spread repetitive sequence PCR (38), was the first PCR-based genome amplification method, which used primers designed to anneal to Alu repeats within the genome. This strategy was further improved to amplify specific DNA flanked by Alu repeats by using the so-called Restricted-PCR technology (44). An alternative method (32), termed the linker adapter technique PCR (LA-PCR), involved restriction digestion of the DNA and ligation of adaptors to serve as priming sites for subsequent PCR. In principle the ligation mediated PCR (LMP) is very similar to the LA-PCR method (32, 33). Nonetheless, this approach has not been widely applied, likely due to technical difficultes involved. PCR-based genome amplification methods, primer extension preamplification (PEP) (34, 35) and DOP-PCR (36, 37) techniques have been developed for the amplification of genomic DNA starting from as little as a single cell. The original PEP protocol involves a 50 cycle PCR program using a 15 bp long oligonucleotide primer; however, via this approach only ~78% of the genome from a single haploid cell can be copied (34).

DOP-PCR and PEP protocols amplify DNA in an exponential fashion, making them highly susceptible to biases, and they have a tendency to specifically over-represent or down-

represent certain sequences. The major disadvantage of PCR-based protocols is that this could distort the ratio of the starting genomic imbalances (45). Recently, Wang et al. have described a modified DOP-PCR protocol for balanced amplification of genomic DNA (46), however the amplification status has not been followed during PCR. In their protocol genomic DNA was digested with a restriction enzyme and tagged linkers were ligated to the products before amplification.

5.3.2.1. Degenerate oligonucleotide-primed PCR

The DOP-PCR technique is increasingly being applied for simultaneous amplification of multiple loci in target DNA using oligonucleotide primers of partially degenerate sequences (36); however, the amplified DNA does not cover the genome completely. Contrary to other PCR-based amplification methods (Alu-PCR, IRS-PCR), DOP-PCR is a species-independent technique. The protocol is adapted for the use of microdissected, formalin-fixed and paraffin-embedded tissue in comprehensive genetic analyses (47).

As is shown in Figure 1/a, primers used for DOP-PCR contain a variable binding region with a sequence of six randomly combined nucleotides which is flanked by a stringent primer binding region at the 5'-end (ten nucleotides) and a main primer binding region at the 3'-end (six nucleotides) which defines the specificity of the reaction.
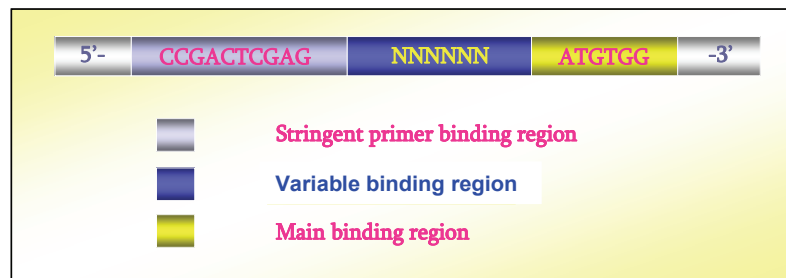
Figure 1/a Sequence of the DOP-PCR primer

The amplification procedure is divided into two steps (Figure 1/b). During the first step, eight PCR cycles are performed at low stringency conditions (annealing temperature, Ta: 30°C). These conditions allow a frequent annealing of the DOP primer, which is primarily mediated by the short specific sequence at its 3'-end and by the adjacent central cassette of degenerated nucleotides. Eventually a pool of many different DNA sequences is generated which should represent a statistically distributed subpopulation of the genomic DNA. During the second step a more stringent annealing temperature is applied and the annealing

temperature is raised to 62°C, allowing amplification only after specific base pairing of the full length primer sequence. After complete DOP-PCR reaction, a high amount of similar DNA fragments will be generated with DOP-primer sequences at both ends.
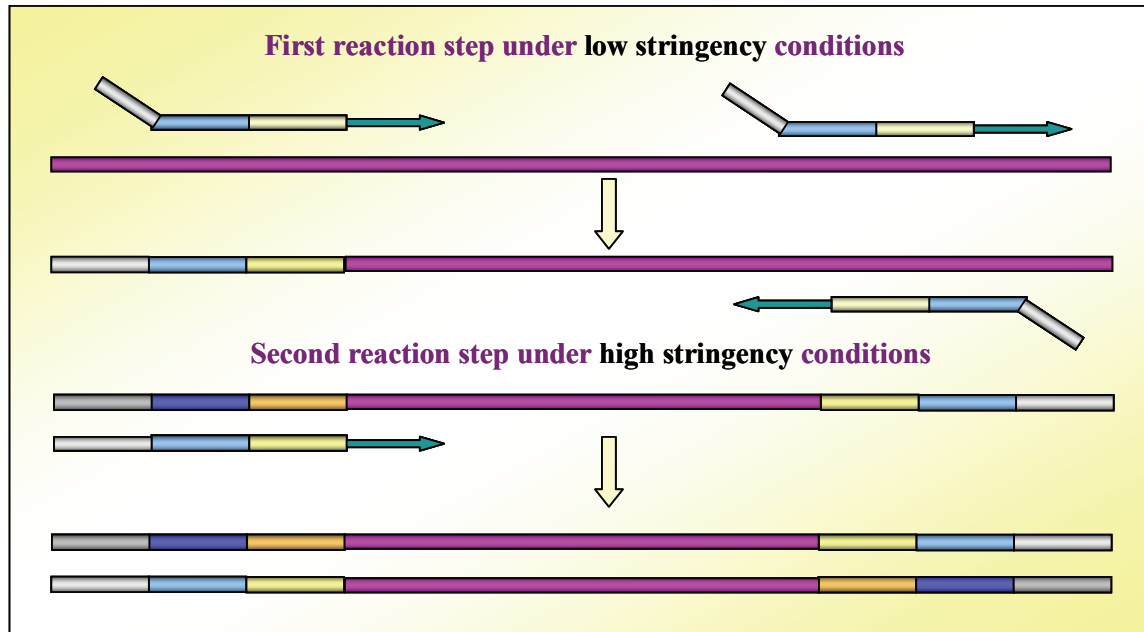
Figure 1/b Reaction mechanism of DOP-PCR

In our improved protocol of DOP-PCR, direct amplification of genomic DNA can be performed without any pretreatment of the samples. Our protocol includes QRT-PCR to follow the cycling status which results in a more reliable and reproducible sample amplification.

DOP-PCR is a simple method for whole genome amplification in comprehensive genetic studies (21) such as metaphase CGH (4), array CGH (48), SNP genotyping (49), microsatellite genotyping (5), SSCP (6), loss of heterozygosity (LOH) (50), and sequence analysis (10), that is increasingly being applied for simultaneous amplification of multiple loci in target DNA. DOP-PCR utilizes oligonucleotide primers with partially degenerate sequences close to their 3' end (36). DOP-PCR is a species-independent approach, which produce sufficient amounts of DNA for analysing clinical tumour samples, for prenatal diagnosis and for many other investigations. A comparison of several DOP-PCR methods is also described by Larsen et al. (47). Not only the amount but also the quality of genomic DNA obtained from various samples is impediment for further studies. For example, paraffin-embedded tissues often provide partially degraded low-quality DNA. Unfortunately, PCR-

based protocols often result in misrepresentation of the genome, with some regions over-represented or even lost. The reliability of PCR-based amplification mostly depends on the exponential phase during cycling. At the late cycles of amplification, the original copy number of chromosomal regions can be changed and the method provides false results. The plateau effect (51, 52) is the result of a marked shift of the overall mass balance in favor of the reaction product. Different factors seem to be responsible for the attainment of the plateau rather than a single factor or parameter, as re-addition of presumably exhausted reagents at late cycles did not cause the reaction to proceed with increased efficiency (53). The plateau effect is caused by the accumulation of product molecules, usually it is the consequence of the significant degree of annealing between complementary strands of the products, rather than between the primers and template. Furthermore, the finite amount of enzyme molecules present is unable to extend all the primer-template complex in the given extension time (54).

5.4. DNA microarray techniques and comparative genome hybridization

5.4.1. DNA microarray technology

Microarray technologies as a whole provide new tools that transform the way scientific experiments are carried out. In place of conducting experiments based on results from one or a few genes, while microarrays allow for the simultaneous interrogation of hundreds or thousands or tens of thousands of genes.

Microarrays are microscope slides that contain an ordered series of samples (DNA, RNA, protein, tissue). The type of microarray depends upon the material placed onto the slide: DNA microarray, RNA microarray; protein microarray; and tissue microarray. Since the samples are arranged in an ordered fashion, data obtained from the microarray can be traced back to any of the samples. This means that genes on the microarray are addressable. The number of ordered samples on a microarray can reach up to a hundred thousand. A typical microarray contains several thousands of addressable genes. DNA printed or spotted onto the slides can be chemically synthesized long oligonucleotides or enzymatically generated PCR products. The slides contain chemically reactive groups (typically aldehydes or primary amines) that help stabilizing the DNA onto the slide, either by covalent bonds or electrostatic interactions. An alternative DNA chip technology allows the DNA to be synthesized directly onto the slide itself by a photolithographic process. This process has been commercialized and is widely available.

DNA microarrays are used to determine the expression levels of genes in a sample (expression profiling) and have been highly successful in a variety of genomic analyses (55), ranging from the detection of SNPs (56) to functional genomics (57-59). Furthermore, DNA microarrays can be used to detect and map copy number changes in regions of the genome.

5.4.2. Development of CGH method

CGH is an in situ hybridization technique used to characterise chromosomal abnormalities where there is a loss (deletion) or gain (amplification) of genetic material (4). It is based on the competitive hybridization of labelled tumour DNA and normal DNA to normal metaphase chromosomes. CGH is not useful for the detection of balanced translocations or inversions where there is no overall gain or loss of material. The main advantage of CGH compared with conventional cytogenetics is that it is not necessary to obtain metaphase chromosome spreads from the tumour under investigation. Thus, CGH is ideally suited to the analysis of samples where it is difficult to obtain good quality metaphase chromosomes. Unlike conventional cytogenetics, CGH is applicable to the study of archival tumour specimens (frozen and paraffin). Recently, using a DOP-PCR method it has been possible to amplify sufficient DNA for CGH even from minute amounts of starting material and in turn this means that CGH can now be regularly performed on microdissected samples. It is now possible to microdissect small pre-malignant lesions and to begin to unravel the genetic changes that might characterise the early changes leading to malignancy.

5.4.3. CGH combined with microarray technique

CGH has already showed a significant impact on the field of cancer cytogenetics as a powerful tool for detection of chromosome copy number aberrations even in epithelial solid tumours, in the case of which it is hard to elucidate tumour specific genome alterations by conventional cytogenetic methods. However, the resolution of CGH to metaphase chromosomes can provide only limited resolution at 5-10 Mb level for detection of copy number losses and gains, and at 2Mb for amplifications. To circumvent this limitation, an innovative strategy, called matrix-CGH (60) or array-based CGH (61) has been devised. CGH using cDNA microarray was also reported to be useful for detection and mapping of gene amplification and homozygous deletions (62). In array CGH, chromosomal targets are replaced by arrays consisting of well-defined genomic clones such as BAC, PAC or cosmid

clones, which are spotted onto a microscopic slide-glass using robotic devices. Since the clones spotted on slide-glass contain sequence information directly connecting with the genome database, we can easily obtain particular biological aspects of genes mapped within regions involved in copy number aberrations detected by array-CGH, facilitating identification of genes responsible for cancer.

5.5. Molecular pathomechanism of different tumour types

5.5.1. Merkel cell carcinoma

The Merkel cells are found in the skin and in those parts of the mucosa derived from the ectoderm (63). These cells are the origin of a rare, malignant neuroendocrine tumour that occurs predominantly in the sun-exposed areas of the skin called MCC (64-70). Local reccurence, and regional or distant metastasis generally develop within a short period of time. Oropharyngeal metastasis is very rare, and metastasis to the palatine tonsil has been described in only one case (71). A perioral or intraoral localization of the MCC is very infrequent: (64, 72) to date, 10 cases of MCC of the lip (73) and 14 cases of intraoral MCCs have been described (64, 74, 75). During the past decade, our co-workers at University of Szeged treated and followed up an elderly woman with MCC of the upper lip. After a long tumour-free period, an anaplastic carcinoma with neuroendocrine features developed in her palatine tonsil, raising the possibility of a late haematogenous metastasis, a second field tumour, or a second primary tumour.

The term "secondary field tumour" was introduced in 1953 by Slaughter et al. who examined slides from patients with head and neck cancer (76). It was observed that all of the epithelium beyond the margins of the tumours displayed histologic alterations, and 11% of the patients were found to have more than one independent area of malignancy. The authors concluded that the mucosa of the head and neck had undergone a change, perhaps due to carcinogen exposure, and was therefore more susceptible to the development of foci of malignant transformation. Organs in which field cancerization has been described since then are the oral cavity, oropharynx, larynx, lung, oesophagus, colon, skin, vulva, cervix, breast, renal pelvis, ureter and bladder (77-80).

The determination of molecular patterns of first and second tumours has become a valuable tool to explore the relationship between them: similar aberrations indicate a metastasis, partly different aberrations indicate a second field tumour, and different

aberrations denote a second primary tumour (78-80). We identified the molecular patterns with CGH with microarray technology. Array-based CGH consists of a series of mapped artificial bacterial chromosomes or sequenced human cDNA clones on glass slides, to which DNA from test and control samples is hybridized (81-83).

Previous CGH studies of MCCs have identified divergent regions that are affected, with a small number of similarities between the samples analysed. Recurrent chromosomal imbalances detected by CGH analysis were loss of 3p, 4p15-pter, 10q, 13q and 17p and gains of 1q, 3q, 5p, 6, 8q, 18 and 20 (84-87). In this study, we detected some of the previously found regions and also numerous novel regions with chromosomal imbalances.

5.5.2. Classification of the thyroid carcinomas

There are four types of thyroid cancer some of which are much more common than others: Papillary and/or mixed papillary/follicular thyroid carcinoma (PTC) (78%); Follicular and/or Hürthle cell (FTC) (17%); Medullary (4%); Anaplastic (ATC) (1%). Thyroid cancer can occur in any age group, although it is most common after age 30 and its aggressiveness increases significantly in older patients. The majority of patients present with a nodule on their thyroid and far less than 1% of all thyroid nodules are malignant.

5.5.2.1. Papillary and anaplastic thyroid carcinoma

The most frequent thyroid cancer is PTC, and this type is one of the most curable cancers with ten year' survival rates (at about 80-90%). Cervical metastasis (spread to lymph nodes in the neck) are present in 50% of small tumours and in over 75% of the larger thyroid cancers. The presence of lymph node metastasis in these cervical areas causes a higher recurrence rate but not a higher mortality rate. Distant metastasis (spread) is uncommon in PTC, but during follow-up 6 to 11% of PTC patients develop distant metastases. Although patients may live for long time with distant metastases, this does significantly worsen prognosis. About one-third of patients with distant metastases survive for 10 years. That is two-third of them die in ten years. An other form of aggressive disease outcome is local recurrance and invasion. Age is important for both predicting development of distant metastases and for influencing long-term survival.

The least common type of thyroid cancer is ATC which has a very poor prognosis. ATC tends to be found after it has spread and is not cured in most cases. Anaplastic tumour has a

very low cure rate and most patients with ATC do not live one year from the day they are diagnosed. ATC often arises within a more differentiated thyroid cancer or even within a goiter. It seems a generally accepted hypothesis, that they originated from differentiated thyroid cancers. Cervical metastasis (spread of the cancer to lymph nodes in the neck) are present in the vast majority (over 90%) of cases at the time of diagnosis. The presence of lymph node metastasis in these cervical areas causes a higher recurrence rate and is predictive of a high mortality rate. Anaplastic cancers invade adjacent structures and metastasize extensively to cervical lymph nodes and distant organs such as lung and bone.

5.5.2.2. Diagnostic molecular markers in papillary and anaplastic thyroid carcinomas

Tumour markers can be used to screen a healthy population or a high-risk population for the presence of cancer, to make a diagnosis of cancer, to determine the prognosis of the patient, or to monitor the course in a patient during follow-up. Several studies have investigated tumour markers in PTC, and some studies have reported them as promising for predicting prognosis, but no warranted markers for PTC have been established. At present thyroglobulin is the only tumour marker of PTC being routinely used to determine the effectiveness of thyroid cancer treatment and to screen for recurrence.

To identify prognostic genetic markers (polymorphic microsatellites, SNPs, changes in gene expression or in gene copy number) which are associated with poor prognosis has been in the focus of several studies. Recently Siironen and co-workers analyzed the expression of COX-2, MMP-2, VEGF-C, Bcl-2, Ki-67 and p21 by immunohistochemistry in 72 samples (36 with aggressive and 36 with benign form) (88), and Gerdes et al. have demonstrated that Ki-67 expression associated with tumour grade and number of mitoses (89). None of these proteins showed superior classification over TNM. Therefore more studies and more robust techniques are needed to predict the progression of the agressive form.

The frequency of LOH on each chromosome arm was determined in 24 patients samples with poor prognosis and in 45 survived cases by Kitamura et al. (90). They found significantly higher frequencies of LOH on 1q, 4p, 7q, 9p, 9q and 16q loci among the poor outcome patient population, however finer resolution of possible genetic markers were not identified. Loss of heterozigocity at the TPO gene locus has been implicated as a cause of the organification defect typical of benign and malignant thyroid tumours (91, 92). Amplification

of the phosphatidylinositol 3-kinase (PIK3CA) gene is relatively common and may be a novel mechanism in activating the PI3K/Akt pathway in some thyroid tumours (93).

All three RAS genes (NRAS, KRAS, HRAS) can be mutated in PTC (94), and Ras mutations and RET/PTC rearrangements are associated with aggressive tumour phenotypes (95-99). The RET gene is found to be rearranged in approxymately 40% of PTCs (100-103). Some authors have desribed BRAF mutation in thyroid tumours (104-110). The majority of ATCs with papillary components are derived from BRAF-mutated PTC, and this indirectly supports the notion that PTC with RET/PTC rearrangements do not progress to ATC. RET/PTC rearrangements activate multiple downstream signaling pathways, including the RAS-RAF-MAPKK-MAPK pathway, do not progress to ATC; whereas PTC with BRAF mutation which activates fewer signaling pathways than RET/PTC, can progress to ATC (111). Expression of RET/PTC1 and RET/PTC3 oncogenes was identified in both benign and malignant studies (112), while RET protein expression has been evaluated in PTCs (113). TRK gene chromosomal rearrangements are found in 10% of PTCs (114, 115). The tumour suppressor gene, p53, is rarely mutated in well differentiated PTC and FTC, but is mutated at a moderate rate in poorly differentiated PTC and at a very high rate in ATC (116-119) but not in its PTC precursor. This indicates that development of ATC is due to further p53 mutation in the setting of an oncogenic mutation such as BRAF (111).

Since no ideal examination method or protocol has been developed by which the circumstances of development and outcome of PTC were able to be defined exactly – which is necessary for the use of aimed therapeutic medicine –, we performed CGH-array analysis of a primary- and terminal-stage APTC, comparing it to GPTC obtained from paraffin-embedded tissue to identify gene copy number alteration as markers which might predict the outcome of an individual patient better than done by TNM classification alone.

5.5.3. The effect of αIIbβ3 integrin on increased angiogenesis and tumour growth in melanoma

Progression of human melanoma is a highly efficient process compared to other malignant tumours since a few millimeters thick tumour (a very small primary in the case of other malignancies) can colonize regional lymph nodes or visceral organs. It is therefore extremely important to understand the molecular mechanisms behind this highly aggressive behavior. Previous studies indicated that the autocrine growth regulation of melanoma

acquired at the switch from a less invasive radial to a more invasive vertical growth phase involves bFGF expression (120, 121).

Some studies have demonstrated that increased expression of αvβ3 integrin in activated endothelial cells promotes angiogenesis and its blockade promotes endothelial cell apoptosis (122-124).

Integrins are ubiquitous transmembrane α/β heterodimers that mediate diverse processes requiring cell-matrix and cell-cell interactions such as tissue migration during embryogenesis, cellular adhesion, cancer metastases, and lymphocyte helper and killer cell functions (125). Platelets express 3 members of the ß$_1$ subfamily (αIIβ1, αvβ1, and αv1β1) that support platelet adhesion to the ECM proteins collagen, fibronectin, and laminin, respectively (126-129), and both members of the β3 subfamily (αvβ3 and αIIbβ3). Although αvβ3 mediates platelet adhesion to osteopontin and vitronectin in vitro (130, 131), it is uncertain whether it plays a role in platelet function in vivo. By contrast, αIIbβ3, a receptor for fibrinogen, vWF, fibronectin, and vitronectin, is absolutely required for platelet aggregation. Because αIIbβ3 plays an indispensable role in hemostasis and thrombosis, it is among the most intensively studied integrins. Expression of αIIbβ3 is restricted to cells of the megakaryocyte lineage. In megakaryocytes, αIIbβ3 is assembled from αIIb and β3 precursors in the endoplasmic reticulum (132) and undergoes posttranslational processing in the Golgi complex, where αIIb is cleaved into heavy and light chains (133). αIIbβ3 can support the adhesion of unstimulated platelets to many of its ligands when they are immobilized in vitro, platelet stimulation is required to enable αIIbβ3 to mediate platelet aggregation by binding soluble fibrinogen and vWF (134).

Different integrins may crosstalk with each other, thereby regulating each other's function. For instance αIIbβ3-mediated signaling in CHO cells influences β1 integrin-mediated cell adhesion and spreading (135). This phenomenon of transdominant signaling appears to involve MAPK activity. Activation of myosin light chain and lipid kinases by the MAP kinase pathway and the Rho family of GTPase is modulated by integrin activity, which provides a link between the extracellular matrix and effect on cell shape and motility that ultimately influences tumour cell invasion. Although the relationship between integrin receptors and metastasis is variable, an increase in β3 integrin expression directly correlates with progression of melanoma (136, 137).

Studies have demonstrated that the megakaryocyte specific αIIbβ3 integrin is expressed in cultured cell lines derived from solid tumours and this integrin is expressed both *in vitro* and *in vivo* (138-144). Compared to expression of αvβ3, expression of αIIbβ3 is much lower and decreases with cell culture *in vitro* (145).

The αIIbβ3 integrin (GpIIbIIIa) is the predominant adhesion receptor of platelets and the expression of the integrin αIIb chain is megakariocyte-specific. It is involved primarily in platelet activation, since it is expressed in a low affinity state and binds fibrinogen only upon activation. The illegitimate expression of αIIbβ3 integrin in human melanoma has been described (146, 147), involved in the same phases of tumour progression as αvβ3.

The transduction of αIIbβ3 into αvβ3-expressing human melanoma cells did not affect the in vitro growth, but promoted the in vivo growth of tumour cells due to decreased apoptosis (147). We have postulated that one possible factor behind the increased in vivo growth is vascularization. Therefore, we have analysed the gene expression changes of αIIbβ3-transfected human melanoma clones with special attention to their angiogenic phenotype.

VI. MATERIALS AND METHODS

6.1. Tissue specimen and genomic DNA isolation

6.1.1. Samples for the improved DOP-PCR technique

Melanoma tissues were obtained from the Department of Dermatology, University of Debrecen, Hungary. Primary melanoma (location: face) and metastatic tumour (location: lymph node) were removed from the same patient at the same time. The relative amount of tumour cells was a minimum of 70% in all lesions as confirmed after hematoxylin and eosin staining by light microscopy. High–molecular-weight DNA was extracted according to a standard procedure starting from 50 mg of tissue (46, 148). Chromosomal CGH and image analyses were performed as described earlier in details elsewhere (148).

Epidermoid, bronchioloalveolar lung carcinoma, 2 renal cell carcinoma, and 2 colorectal carcinoma specimens were obtained from the Institute of Pathology, Szeged University. Conn and Cushing adenoma samples were obtained from Semmelweis University, Budapest. DNA was purified by using the DNA purification kit from Macherey-Nagel (Düren, Germany) according to the manufacturer's instructions.

6.1.2. Samples for the Merkel cell carcinoma study

Between 1970 and 2003, 4418 patients with malignant orofacial tumours were treated in Department of Dentistry and Oral Surgery at University of Szeged. One of these patients suffered from MCC. A 79-year-old Caucasian woman presented with a tumour in her upper lip. She was an outdoor worker and never smoked. She was disturbed only about the aesthetics. The physical examination revealed a 2–3-cm firm, compact mass in the skin of the upper lip on the left side. It was sharply separated from its surroundings and had a teleangiectatic surface (Figure 2).

Figure 2. MCC developed in the skin of the upper lip

The tumour was classified as stage T2. No regional lymph-node metastasis was detected. Surgical resection of the tumour and removal of the regional lymph nodes were suggested, but she refused it. As an alternate therapy, a biopsy was taken, and cryotherapy was applied according to the standard protocol. The histological and immunohistochemical characterization was done in the Department of Pathology at Medical University of Szeged. Light microscopy revealed that the tumour was confined to the dermis and was sharply separated from the epidermis. The tumour cells were arranged in nests and cords. Cytologically, the tumour cells were monomorphic, the nuclei were round and the chromatin pattern was finely granular and "dusty". The nucleoli were small; often two or even three were detected. The cytoplasm was scanty. The mitotic rate was high (six to ten figures/ high-power field). The Grimelius staining was negative. The results of immunostainings are shown in Table 1. The histological and immunohistochemical features pointed to MCC of the lip. Following the histological diagnosis, distant metastases in the lungs and bones were searched for, with negative results.

Immunohistochemical markers	Lip tumour	Tonsillar tumour
AE1/AE3	+++	+++
Cytokeratin	20	20
Paranuclear dots	+++	++
Chromogranin	++	+
Synaptophysin	-	-
TTF	-	-
HMB-45	-	-
CEA	-	-
Lymphoid markers	-	-

Table 1. Immunohistochemical findings

In the 7-year follow-up, the patient was in a tumour-free condition. After 7 years, she was admitted to the County Hospital in Kecskemét with a left palatine tonsillar tumour. This tumour was resected in part, and the regional lymph nodes were removed. Histologically, the tumour displayed features of anaplastic carcinoma.

The morphological appearance of the tumour resembled that of the MCC of the lip. A further excision was performed 3 months later. The morphological and immunohistochemical

features of the tonsillar tumour were essentially the same as observed 3 months earlier. The patient died at home on the 20th postoperative day. Autopsy was not performed.

Paraffin-embedded tumour tissues and unaffected lymph nodes (200-500 mg) were deparaffinated in hexane, and washed with ethanol. DNA was purified by using the DNA purification kit from Macherey-Nagel (Düren, Germany) according to the manufacturer's instructions.

6.1.3. Papillary thyroid carcinoma samples

PTC was detected in a 63-year-old male patient; carcinoma was confirmed by cytology and other investigations. Total thyreoidectomia and lege artis ablatio with ^{131}I were performed; unfortunately, after eight months, local recidiva developed. A necessary reoperation was carried out by the University of Debrecen; despite the operation, however, the tumour spread into the pharynx, main vessels, and pleura, and the patient died three months later. On the basis of histology results, anaplastic dedifferentiation was detected. The primary- and terminal-stage APTC samples obtained from the above patient were analysed compared GPTC and normal thyroid tissue in further QRT-PCR studies. The disease course of the female patient with GPTC providing control samples in some experiments was followed strictly for five years after operation and radioiodine ablation.

Other PTC samples included in further studies and normal thyroid tissues were obtained from the Department of Pathology University of Debrecen, Jósa András County Hospital in Nyíregyháza, Erzsébet Hospital in Hódmezővásárhely, County Hospital in Kecskemét and Pándy K County Hospital in Gyula. Two disease course groups of our cases were created: the GPTC (group A): patients with no recurrance and no metastases, all of them are disease free up to now. There were 10 patients of GPTC, all of them were female. Mean age was 42.1 years (range: 27-52 years) at the time of the operation. Median follow-up was 4.8 years (range: 3-7). The second group was the I/APTC (group B) (14 intermediate – i.e. metastasis developed only in cervical lymph nodes, by which the survival rate is much higher than by APTC, and 10 malignant APTCs. This group B consisted of 24 patients (17 female, 7 male). Patients with cervical (12) and regional (mediastinal) lymph node (2), pulmonary (6), bone (3) metastases, trachea infiltration (1), and local invasion (4) in different combination. The mean age of patients of the I/APTC group was 48.3 years (range: 13-76 years) at the time of the operation. Median follow-up was 6.8 years (range: 9 months-17 years). Eight of them died, and the mean survival time following operation was 5.6 years (range: 9 months-22 years).

Paraffin-embedded tissues (500 mg) were deparaffinated in hexane and washed with ethanol. DNA was purified by the DNA purification kit from Macherey-Nagel (Düren, Germany), according to the manufacturer's instructions.

6.2. DNA and RNA quantity measurement

The quantity of genomic DNA and total RNA was assessed spectrophotometrically by NanoDrop (Rockland, DE, USA). Genomic DNA was used for microarray analysis and for QRT-PCR.

The WM983B cell line that does not express αIIbβ3 on the cell surface was a kindly provided to us by M. Herlyn (The Wistar Institute, Philadelphia, PA). Mock transfected WM983B cells (3.1P) and αIIb and β3 transfected WM983B cells (19L and 19H) have been described in a study by Trikha M. et al. (147). 19H transfected cell line was subcloned by limited dilution to obtain 7D7 and 8F3 subclones. The parental cell line was grown in RPMI-1640 medium supplemented with 5% FBS and antibiotics (Sigma Chemical Co., St. Louis, MO) in a 5% CO_2 humidified atmosphere at 37°C. Transfected cells were maintained in medium containing G418 (Gibco BRL, Gaithersburg, MD).

RNA isolation from $5x10^6$ cells was carried out with the RNA isolation kit of Macherey-Nagel (Düren, Germany) according the manufacturer's instruction. The RNA concentration was assessed spectrophotometrically by NanoDrop (Rockland, DE, USA) and the quality was checked by electrophoresis. RNA was stored at -80°C in the presence 30 U of Prime RNAse inhibitor (Fermentas, Vilnius, Lithuania). Total RNA was used for RT, microarray analysis and for QRT-PCR.

6.3. Quantitative real-time PCR

6.3.1. Preparation of DOP-PCR amplified and overamplified genomic DNA

Genomic DNA (20 ng from native tissue and 100 ng from paraffin embedded tissue) was amplified with a modified version of the DOP-PCR protocol by using a RotorGene 3000 QRT-PCR instrument, (Corbett Research, Mortlake, Australia), to follow the amplification. The DNA concentration was assessed spectrophotometrically by NanoDrop (Rockland, DE, USA). Reactions were performed in a total volume of 100 μl. The cycling parameters were as follows: heat start at 95 ^{o}C (15 min); 8 cycles denaturation at 94 ^{o}C (50 s); annealing for 2 min from 45 ^{o}C to 72 ^{o}C with a 0.2 ^{o}C/s ramp; and, extension at 72 ^{o}C (90 s). After 8 cycles, the reaction mix was divided into two 50 μl aliquots and SybrGreen was added to both (1x final concentration, Molecular Probes, Eugene, USA). The following cycling protocol was

performed in a real-time PCR instrument: denaturation at 95 ^{o}C (40 s); annealing at 58 ^{o}C (60s); and, extension at 72 ^{o}C for 80 s. To avoid over-amplification of the products, cycling was terminated just before the reaction reached the plateau (i.e., at 13-15 cycles); in contrast, the over-amplified genomic DNA was obtained from PCR with 21 cycles.

The PCR products were purified with PCR-purification columns (Bioneer, Daejeon, Korea). In the reactions, UN primer (5'-CCGACTCGAGNNNNNNATGTGG-3') was used in 1 µM concentration (36). The reactions were performed with ExTaq DNA polymerase in 1X buffer (Takara, Tokyo, Japan) in the case of MCC, while the reactions were performed with 1x ABsolute QPCR Mixes (ABgene, Surrey, UK) in case of confirmation of improved DOP-PCR and PTC.

6.3.2. Determination of the differences in relative copy numbers of the genome

QRT-PCR was carried out in a final volume of 20 µl with 20 or 100 ng (DNA obtained from native or paraffin-embedded tissues accordingly) non-amplified or amplified genomic DNA in a RotorGene 3000 instrument (Corbett Research, Mortlake, Australia). The reactions were performed with 5 pmol/each forward and reverse gene-specific primers in 1x ABsolute QPCR Mix (ABgene, Surrey, UK) with SybrGreen (1 µM final concentration, Molecular Probes, Eugene, USA) with the following protocol: heat start for 15 min at 95 °C, 45 cycles of 25 s denaturation at 95 °C, 25 s annealing at 59 ^{o}C and 25 s extension at 72 ^{o}C. Fluorescent signals were collected after each extension step at 72 ^{o}C. Curves were analysed with the RotorGene software, using dynamic tube and slope correction methods, while ignoring data from cycles close to baseline. Primers were designed by using the PrimerExpress software (Applied Biosystems, Foster City, CA, USA). Relative ratios were normalized to the C_t values of the metallopeptidase 1 gene as an internal control - in the case of primary and metastatic melanoma samples confirming improved DOP-PCR technique -, and calculated with the Pfaffl method (149). The sequences of PCR primers used in this study were deposited to http://160.114.60.33/Data1/. All the PCRs were performed three times in separate runs.

6.3.3. Confirmation of CGH–microarray results

The confirmatory QRT-PCR was performed on a RotorGene 3000 instrument with previously described protocol (detailed in the 6.3.2. subsection of this thesis). Relative ratios were normalized to the Ct values obtained with the dihydrofolate reductase gene probe in the case of MCC and alpha1-fetoprotein transcript factor and H3 histone (family 3A) in the case of PTCs and calculated with the Pfaffl method (149). PCR primers used are listed in Table 2. All the PCRs were performed 4 times in separate runs.

Table 2. Sequences of the oligonucleotides (5'-3') used in the case of MCC, tonsillar tumour and thyroid carcinomas

Gene (Accession No.)	Chrom. location	Forward primer	Reverse primer	Product size (bp)
Merkel cell carcinoma and tonsillar tumour				
Steroid 5-alpha-reductase 2 (M74047)	2p23	CAGAAGCCCCAAGCAACTTT	CCTTCTTGAACAGGTCCTGAGAA	69
Hepatocyte nuclear factor-3 alpha (U39840)	14q12-q13	CTCAAGAGTTGCTTGACCGAAA	GGGCCATCTGTGGGTAGAGA	67
Zinc finger protein (AF020591)	19q13.43	GAAATTTCCCTGCCAGACCTT	CATGAAGCCCCACTCTGAGAGT	73
Androgen receptor (dihydro-testosterone receptor) (M23263)	Xq12	CGGAAATGATGGCAGAGATCA	TGGGCTTGACTTTCCCAGAA	66
C8FW phosphoprotein (AJ000480)	8q24.13	GGACGATACCCCTTCCATGA	GTCCACGCCGAATTTGG	61
Cardiac myosin binding protein-C (U91629)	11p11.2	GCCTAAATCCGAGCATCTGTTT	TGCACTCTCAGGGAATTTGAGA	70
EST (N22765)	15q14	CCTGATTCCAGAAAAGCAAGTGT	CACTGAGATTACCGGGCATGA	76
Cytochrome P450, subfamily XIA (M14565)	15q22	CTGGTGCAAGTGGCCATCTA	AATTTTCCGGGTCGAAGAAGA	64
EST sim. to phosphatidylcholin transfer protein (AA933627)	17q23	CACAAGGCTATGCACAAAGCA	GGAAACTGAGGCGTCAAGATG	68
Dihydrofolate reductase (BC070280)	5q14	CTGTCATGGTTGGTTCGCTAAA	TGCCGATGCCCATGTTC	60
Thyroid carcinomas				
Tre-2 (X63547)	17p13	TCCAGCGGCCCATTTG	AGGGCGTGGAAAAACGAGAT	57
Thymosin beta 10 (BC016731.1)	5q31.3	AATCGCCAGCTTCGATAAGG	GGTCGGCAGGGTGTTCTTC	67
Image EST (R78712)	15q25	GGTCATGTGTCGTGAAATATTATTGTT	CCCGGCTGAGATTTTACATTTT	76
Euk. Initiation factor 4EBP3 (AF038869)	5q31.3	ACCTGGCATGTGGAGTTACAGA	TGGATGCCCCAGGAAGAG	70
KIAA0549 (AB011121)	2q33	TTGCCTGGACAGTTCACGTTTCC	AATCGGACAATTTAACGTTGTACTACTC	87
Fibroblast growth factor 7 (M60828)	15q15-q21.1	GAACAAAATTTCTAATGCTGCTCAAG	CATCAATCACTGTTGCTATCTTATATACAAG	93
Alpha 1-fetoprotein transcription factor (U93553)	1q32.1	GGTGTCCAGGAACAAGTCAATG	CTCTGTCTGCTGCGGGTAGTT	71
H3 histone, family 3A (BC081561)	1q41	TGCAGGAGGCAAGTGAGGC	CTGGATGTCTTTTGGCATAATTGTT	101

6.4. Preparation of microarray probes

6.4.1. Preparation of genomic DNA probes for array hybridization of MCC

100 ng purified DNA was labelled with another round of PCR in the presence of Cy3-dUCTP (0.05 mM) in a total volume of 50 µl with the same parameters for 20 cycles as in the second PCR. In all these reactions, UN primer (5'-CCGACTCGAGNNNNNNATGTGG-3') was used in 1 µM concentration. The reactions were performed with ExTaq DNA polymerase

in 1X buffer (Takara, Tokyo, Japan). The labelled PCR products were purified with the PCR purification kit (Bioneer, Daejeon, Korea). The eluted DNA was dried in a Speed-Vacuum.

6.4.2. Preparation of genomic DNA probes for array hybridization of PTC samples

Three microgramms of amplified genomic DNA was fragmented with AluI restriction endonuclease, then it was tailed with dTTP resulting an oligo dT sequence at the 3'-ends of the products. Afterwards, a special capture oligo was ligated to the tailed DNA according to Genisphere DNA labeling system (Genisphere, Hatfield, PA).

6.4.3. Generation of microarray probes for human melanoma cells

Four microgramms of total RNA was reverse transcribed using poly-dT primed Genisphere Expression Array 350 Detection system (Genisphrere, Hatfield, PA) in 20 μl total volume using 20 Unit RNAsin (Fermentas), 1x first strand buffer and 200 Units of RNAse H (-) point mutant M-MLV reverse transcriptase (Fermentas). All the other probe preparation steps were done according the manufacturer's instruction (Genisphere).

6.5. Microarray construction and array hybridization

6.5.1. Human cDNA microarray construction

Construction and use of microarrays were performed as previously described (43, 150). Briefly, 3200 cDNA inserts from human cDNA libraries (melanoma, lymphocytes, heart and mixed tissue libraries) were amplified and purified with MultiScreen-PCR plate (Millipore), resuspended in 50% dimethylsulfoxide/water and arrayed on FMB cDNA slides (Full Moon BioSystems, Sunnyvale, CA) by using a MicroGrid Total Array System (BioRobotics, Cambridge, UK) spotter with 16 pins in a 4 x 4 format. DNA elements were deposited in duplicate. The diameter of each spot was approximately 200 μm. After printing, DNA was UV crosslinked to the slides (Stratagene, Stratalinker, 700 mJ).

6.5.2. CGH-array hybridization in the case of MCC

The labelled DNA was reconstituted in ChipHybe hybridization buffer (Ventana Discovery, Tuchon, USA) containing 20 μg human Cot DNA and 5 μg salmon sperm DNA (Invitrogen). Hybridization was performed on human cDNA microarrays having 3200 gene-specific samples in duplicate in 200 μl by using the Ventana hybridization station (Ventana)

at 42 $^\circ$C for 8 h. (151, 152). After hybridization, the slides were washed twice in 0.2X SSC at RT for 10 min, and then dried.

6.5.3. Array hybridization in the case of thyroid tumours and human melanoma cells

cDNA was hybridized onto human cDNA microarrays in a Ventana hybridization station (Ventana Discovery, Tuchon, State) by using the ''antibody'' protocol. First hybridization was performed at 42°C for 6 hr in ''Chiphybe'' hybridization buffer (Ventana) and then 2.5 µl of Cy5 capture reagents (thyroid tumours), while in other experiments 2.5 µl of each Cy5 and Cy3 capture reagents (MCC investigation) were added to the slides in 200 µl Chiphybe hybridization buffer (Ventana) and incubated at 42°C for 2 hr. After hybridization, the slides were washed in 0.2 x SSC twice at RT for 10 min and then dried and scanned. In the case of thyroid tumours the probe and control samples were hybridized onto separate slides, while they were hybridized onto the same cDNA microarrays in the case of MCC analysis.

6.6. Array data analysis

The presented data were calculated from the results of 4 data points obtained from two separate labelling and hybridization protocols. The slides were scanned with confocal laser scanner (ScanArray Lite, GSI Lumonics, Billerica, MA, USA). Image files were analysed with the GenePix Pro 3.0.5. program (Axon, Union City, CA, USA). The background corrected intensity data was filtered for flagged spots and weak signal. After automatic flagging, manual flagging was performed to exclude spots having irregularities, such as scratches and dust particles. Technical replicates on the same array were averaged. Data were excluded in cases where technical replicates were significantly different. Data obtained by the median of feature pixels were accepted only if 30 % of pixels were above 2 x standard deviation of the background intensity. Normalization was performed using the print-tip LOWESS method (153). Next we used the one-sample t-test in order to determine the genes to be regarded as changed in copy number. Logarithm was taken from each ratio to fulfill the *t*-test's requirement for a normal distribution. Genes for which the mean of log-ratios across the biological replicates was equal to zero at a significance level $\alpha=0.05$ are considered to have an unchanged copy number. On the other hand, genes having a p-value smaller than α and the average-fold change (over- or under-representation) of the four data points were at least 2.0-fold were considered as changes in DNA copy number or gene expression.

VII. RESULTS AND DISCUSSION

7.1. Improved DOP-PCR-based representational whole genome amplification using QRT-PCR

The amount of genomic DNA available for genetic studies can often be limiting. DOP-PCR is an appropriate method for overcoming these limitations by efficiently performing whole genome amplification. We have presented a more reliable PCR-based genome amplification procedure, developed as an alternative sample amplification method which follows the amplification status by QRT-PCR. With real-time detection of the products, DNA over-amplification could be diminished. After initial amplification of the genome, SybrGreen dye is added to the reaction mix and a second amplification step is applied in a QRT-PCR instrument. The cycling is performed until the reaction reaches the plateau (Figure 3).
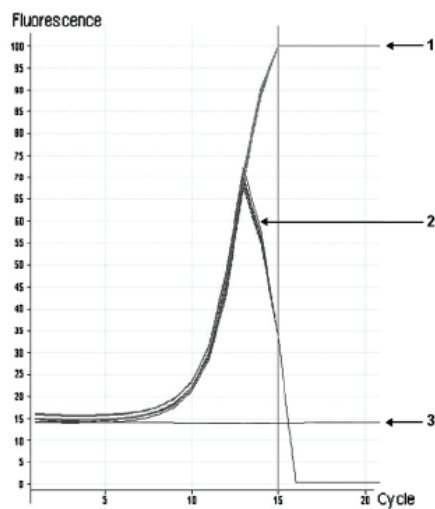
Figure 3. Whole genomic DNA amplification using QRT-PCR. Diagram of the primary, metastatic melanoma tissue and normal peripheric lymphocyte. The amplification halted at the 13th cycle, the amplified genomic DNA (2) was generated in the exponential phase of the reaction; the over-amplified genomic DNA (1) was isolated from reactions halted at the 21st cycle; Number 3 denotes for the non-template control.

To compare the original gene copy number of different templates generated by using the traditional DOP-PCR and with the protocol using QRT-PCR, 44 genes were selected for confirmation by using QRT-PCR analysis in case of two melanoma samples. Genes were selected on the basis of metaphase CGH data performed earlier (154). The QRT-PCR was performed on DNA samples obtained from primary and metastatic melanoma tissues resected from the same patient along with normal DNA prepared from peripheral blood of a healthy individual as a control. Altogether 88 relative copy numbers were determined on three

Table 3. Comparison of copy number changes of several gene loci obtained from primary and metastatic tumour samples relative to normal tissue by using non-amplified and different amplified genomic DNA as templates. Light gray: altered relative copy number at certain chromosomal regions in the amplified sample compared to control, non-amplified sample.

Chrom. Location	Gene product (Acession No.)	Type of melanoma	Non-amplified SD	DOP-PCR+ QRT-PCR SD	DOP-PCR SD	Metaphase CGH
Loss of chromosomal regions						
12q14.3	Chaperonin cont. t-complex polypept. 1b (AF026293)	primary	0,43 (0,21)	0,27 (0,28)	2,20 (0,39)	deletion
		metastatic	0,44 (0,12)	0,27 (0,03)	0,31 (0,13)	
17p13	Human clone 23665 (U90913)	primary	0,50 (0,07)	0,39 (0,03)	0,31 (0,05)	deletion
		metastatic	0,48 (0,01)	0,33 (0,03)	0,48 (0,07)	
17p13.1	15S-lipoxygenase (U78294)	primary	0,50 (0,08)	0,50 (0,06)	1,77 (0,10)	deletion
		metastatic	0,51 (0,02)	0,44 (0,12)	1,44 (0,00)	
2p23	Anaplastic lymphoma kinase (Ki-1) (NM_004304)	metastatic	0,57 (0,03)	0,56 (0,28)	0,28 (0,13)	deletion
10q26.13-q26.3	dedicator of cytokinesis 1 (NM_001380)	primary	0,58 (0,34)	0,52 (0,06)	0,74 (0,05)	deletion
Genes with no change						
2p23	Anaplastic lymphoma kinase (Ki-1) (NM_004304)	primary	1,11 (0,07)	0,68 (0,03)	2,77 (0,95)	no change
2p25.3	Myelin transcription factor 1-like (BC071612)	primary	1,16 (0,09)	0,50 (0,17)	0,74 (0,06)	no change
		metastatic	0,60 (0,01)	0,40 (0,09)	0,54 (0,06)	deletion
10p12.1	G protein-coupled receptor 158 (AY528411)	primary	0,87 (0,06)	0,52 (0,03)	1,47 (0,05)	no change
		metastatic	0,64 (0,06)	0,59 (0,02)	1,25 (0,07)	deletion
9p23-p24.3	Prot. tyrosine phosphatase, receptor D (NM_130392)	primary	0,83 (0,02)	0,53 (0,22)	1,63 (0,93)	deletion
		metastatic	0,85 (0,16)	0,58 (0,25)	0,69 (0,29)	
11p15.5	p27-BWR1B (AF037066)	primary	0,89 (0,06)	0,92 (0,03)	0,90 (0,12)	no change
		metastatic	0,82 (0,31)	1,13 (0,08)	0,72 (0,06)	
11q23	Apolipoprotein A-I precursor (X02162)	primary	0,76 (0,04)	0,86 (0,38)	0,90 (0,12)	no change
		metastatic	0,90 (0,07)	0,82 (0,32)	0,75 (0,10)	
1q23	CD48 antigen (B-cell membrane protein) (M37766)	primary	1,07 (0,11)	0,69 (0,14)	0,48 (0,12)	no change
		metastatic	1,33 (0,18)	0,90 (0,36)	0,49 (0,14)	
9q33.1	astrotactin 2 (BC010680)	primary	1,01 (0,10)	0,49 (0,16)	0,66 (0,25)	no change
		metastatic	1,17 (0,32)	0,59 (0,65)	0,65 (0,15)	
1p31	Leptin receptor (U66497)	primary	0,86 (0,01)	1,10 (0,02)	1,27 (0,23)	no change
		metastatic	0,77 (0,07)	1,03 (0,2)	0,57 (0,05)	
2q35	Fibronectin 1 (X02761)	primary	1,03 (0,11)	0,99 (0,16)	0,99 (0,31)	no change
		metastatic	1,14 (0,17)	1,11 (0,06)	1,24 (1,03)	
5q11.2	Integrin, alpha 2 (M28249)	primary	1,20 (0,19)	0,97 (0,16)	0,48 (0,06)	no change
		metastatic	1,18 (0,20)	0,91 (0,05)	0,35 (0,30)	
7q31	Met proto-oncogene (J02958)	primary	1,05 (0,23)	0,82 (0,07)	0,87 (0,06)	no change
		metastatic	1,31 (0,04)	1,10 (0,03)	0,41 (0,06)	
19q13.3	OTK18 (D50419)	primary	1,18 (0,12)	0,51 (0,02)	1,01 (0,55)	no change
		metastatic	1,03 (0,10)	0,56 (0,01)	0,44 (0,06)	
14q11.2-13.1	Ribonuclease k6 precursor gene (U64998)	primary	1,19 (0,06)	0,80 (0,03)	1,22 (0,15)	no change
		metastatic	1,31 (0,05)	1,11 (0,06)	0,93 (0,12)	
14q22.3-q23.1	Retinoblastoma-binding protein 1 (S66427)	primary	1,24 (0,09)	0,82 (0,01)	1,34 (0,03)	no change
		metastatic	1,43 (0,04)	1,12 (0,16)	0,99 (0,31)	
14q23-24.1	RNA pol. transcriptional regulation mediator (U78082)	primary	1,15 (0,12)	0,71 (0,03)	1,22 (0,10)	no change
		metastatic	1,14 (0,04)	0,89 (0,06)	1,17 (0,10)	
4p14	Ubiquitin carboxyl-terminal hydrolase L1 (X04741)	primary	0,90 (0,14)	0,35 (0,27)	0,62 (0,25)	amplification
		metastatic	0,98 (0,19)	0,60 (0,48)	0,80 (0,04)	
16p12-13.2	Epithelial amiloride-sensitive Na channel g (X87160)	primary	1,23 (0,15)	1,10 (0,11)	1,17 (0,24)	no change
		metastatic	1,30 (0,07)	1,05 (0,11)	1,14 (0,10)	
11q13.1-13.3	Cell cycle checkpoint control protein (U53174)	primary	1,03 (0,13)	0,84 (0,20)	0,67 (0,13)	no change
		metastatic	1,14 (0,13)	0,97 (0,14)	0,63 (0,03)	
15q23-25	Neuromedin B precursor (M21551)	primary	1,35 (0,13)	1,31 (0,14)	2,27 (2,07)	no change
		metastatic	1,22 (0,10)	1,42 (0,05)	2,16 (1,91)	
15q15-q21.1	Fibroblast growth factor 7 (M60828)	primary	0,89 (0,12)	0,68 (0,11)	0,91 (0,02)	no change
		metastatic	0,82 (0,10)	1,02 (0,05)	0,48 (0,06)	
16p13.3.	N-methylpurine-DNA glycosylase (M74905)	primary	1,28 (0,04)	2,00 (0,17)	0,82 (0,11)	no change
		metastatic	1,34 (0,12)	1,73 (0,03)	0,78 (0,15)	
19q13.3-4	Electron-transfer-flavoprotein b (X71129)	primary	1,24 (0,06)	1,12 (0,10)	0,99 (0,41)	no change
		metastatic	1,11 (0,04)	0,93 (0,18)	0,45 (0,06)	
1p33-34.1	Mitotic centromere-associated kinesin (U63743)	primary	1,05 (0,18)	0,67 (0,01)	0,50 (0,06)	no change
		metastatic	1,03 (0,11)	0,83 (0,07)	0,51 (0,02)	
2q32-33	amyotrophic lateral sclerosis 2 (AB011121)	primary	1,10 (0,37)	1,37 (0,09)	1,41 (0,11)	no change
		metastatic	1,11 (0,22)	1,31 (0,05)	0,75 (0,24)	
14q31	Galactocerebrosidase (D86181)	primary	1,46 (0,12)	0,68 (0,10)	0,50 (0,01)	no change
		metastatic	1,41 (0,04)	0,87 (0,08)	0,55 (0,08)	
15q25	Image EST R78712 (R78712)	primary	1,22 (0,09)	0,76 (0,03)	0,68 (0,25)	no change
		metastatic	1,22 (0,17)	0,91 (0,03)	0,65 (0,05)	
2q31.1	Recepin (U03644)	primary	0,96 (0,00)	0,60 (0,08)	0,82 (0,11)	no change
		metastatic	0,91 (0,25)	1,00 (0,00)	1,01 (0,05)	
20q13.12	Image EST 364782 (AA034412)	primary	1,25 (0,11)	0,49 (0,02)	1,11 (0,34)	no change
		metastatic	1,40 (0,12)	0,50 (0,07)	1,31 (0,03)	
3p12	Roundabout, axon guidance receptor (BC057243)	primary	1,20 (0,06)	1,31 (0,04)	0,80 (0,11)	no change
		metastatic	1,13 (0,07)	0,97 (0,24)	2,89 (0,12)	amplification
7p15	CG1 (U97198)	primary	1,14 (0,13)	0,79 (0,05)	1,71 (0,30)	amplification
4p14	Amyloid beta precursor prot. binding B2 (BC027946)	primary	1,03 (0,11)	1,49 (0,07)	0,55 (0,11)	amplification
3q26.31	N-acetylated a-linked acidic dipeptidase 2 (AF040990)	primary	1,34 (0,09)	1,05 (0,17)	1,65 (0,40)	no change
Gains of chromosomal regions						
7p15	CG1 (U97198)	metastatic	1,52 (0,08)	0,92 (0,00)	2,63 (0,78)	no change
4p14	Amyloid beta precursor protein-binding B2 (BC027946)	metastatic	1,50 (0,13)	1,51 (0,08)	0,81 (0,03)	amplification
10q26.13-q26.3	dedicator of cytokinesis 1 (NM_001380)	metastatic	1,52 (0,07)	0,43 (0,00)	0,86 (0,24)	deletion
3q26.31	N-acetylated a-linked acidic dipeptidase 2 (AF040990)	metastatic	1,56 (0,06)	1,67 (0,18)	1,09 (0,15)	amplification
1p36.21	Cardiodilatin-atrial natriuretic factor (AL021155)	primary	1,80 (0,21)	0,80 (0,04)	1,14 (0,19)	amplification
		metastatic	2,08 (0,20)	0,86 (0,09)	1,48 (0,02)	
6p25.2	Cell death protein (RIP) (U50062)	primary	1,71 (0,05)	1,60 (0,32)	1,23 (0,16)	amplification
		metastatic	1,58 (0,05)	1,69 (0,31)	2,33 (0,28)	
18q21.3-q22	UV-B repressed sequence, HUR 7 (X98307)	primary	1,56 (0,15)	1,91 (0,03)	1,74 (0,03)	no change
		metastatic	1,54 (0,12)	2,48 (0,65)	0,71 (0,38)	
6p12.2	Polycystic kidney, hepatic disease 1 (AY074797)	primary	1,61 (0,21)	1,64 (0,17)	1,09 (0,10)	amplification
		metastatic	1,62 (0,21)	1,72 (0,62)	0,85 (0,07)	
17q11.2-q12	Amiloride-sensitive cation channel 1(BC075043)	primary	3,12 (1,10)	1,61 (0,05)	1,69 (0,22)	amplification
		metastatic	2,02 (0,40)	1,49 (0,12)	0,95 (0,20)	
17q23	Breast carcinoma amplified sequence 3 (BC001250)	primary	1,69 (0,06)	1,74 (0,04)	4,23 (1,98)	amplification
		metastatic	2,08 (0,22)	2,14 (0,06)	0,62 (0,02)	
5q21.3	F-box, leucine-rich repeat protein 17 (BC063316)	primary	1,75 (0,03)	1,65 (0,02)	4,77 (2,47)	amplification
		metastatic	2,64 (1,08)	2,46 (0,67)	1,73 (0,56)	

different templates: non-amplified as control, amplified with DOP-PCR and ampified with our protocol: DOP-PCR in combination with QRT-PCR (Figure 3). In traditional DOP-PCR protocol we applied 21 cycles for each reaction, however genomic DNA was PCR amplified with our combined DOP-PCR-QRT-PCR method in 13-15 cycles, which were sufficient to reach early saturation phase. The copy numbers of selected genes were normalised to the copy number of the metallopeptidase 1 gene. This single copy gene did not show any alteration in copy number in either melanoma sample and gave reproducible results in all cases. Relative copy number change resulted being less than 0.5 meant loss of genetic material (heterozygous loss). If this value was greater than 1.5, it was defined as gain or gene amplification at that certain chromosome location (duplication of one allele). The results of the confirmatory QRT-PCR are shown in Table 3.

Genomic changes (no change, loss or gain of copy number) were determined for all the 44 genes in each method on both samples (primary melanoma and metastatic tumour) and all the 88 values were compared to each other. In case of the QRT-PCR protocol 88.6% of the copy number changes matched the non-amplified samples, while traditional DOP-PCR resulted in only 63.6% accuracy. The correlation coefficient for the comparison of the non-amplified and the DOP-PCR amplified genomic DNA was only 0.27, while this value was significantly increased to 0.65 when the same protocol was used, but the amplification status was followed by QRT-PCR.

To demonstrate the differences in relative copy numbers, which were obtained with different amplification methods, a scatter plot was prepared (Figure 4). In case of our combined method most of the genes had relative copy numbers similar to those of the non-amplified method, while traditional DOP-PCR distorted the relative copy numbers detected in the non-amplified samples.

To strengthen the extension of the preliminary observations a larger number of tumour types were further analysed. Amplified samples from epidermoid, bronchiolo-alveolar lung carcinoma, two renal cell carcinoma, two colorectal carcinoma, Conn and Cushing adenoma samples were processed as described above. Copy number changes of eight different chromosome regions were followed by QRT-PCR. Non-amplified and amplified samples obtained from traditional DOP-PCR technique and from our improved protocol were analysed. The results of copy number changes can be seen at http://160.114.60.33/Data2/.
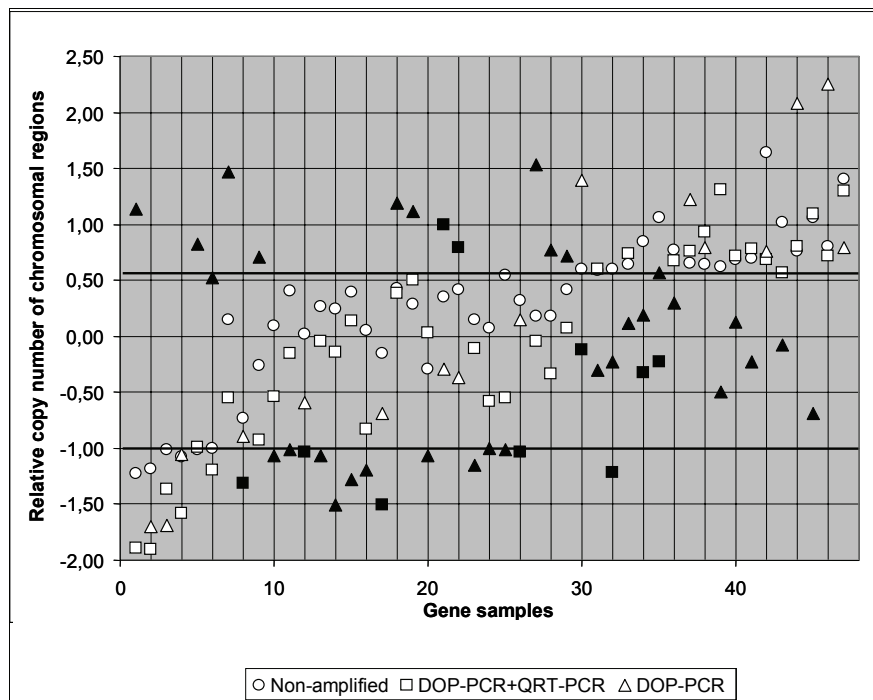
Figure 4. Scatter plot of relative copy number of genes in primary and metastatic melanoma samples obtained with three different protocols. Values of copy number changes are in $\log_2$ scale. Only those genes were selected of which the values by any of the protocols were above +0.58 and below -1. The black squares and triangles mean those values which are different from the relative copy numbers of non-amplified samples.

In the case of the analysed eight tumour samples there was 84.4% concordance in copy number alterations between the QRT-PCR protocol and the non-amplified samples, while this value was only 64.0% for the traditional DOP-PCR (Figure 5).

Figure 5. Comparison of relative copy number of amplified samples genes to the original copy number (■: change in original copy number of genes □: no change in original copy number of genes)

In conclusion, our method improved the traditional DOP-PCR technique for whole genome amplification. Improved reliability of the QRT-PCR-controlled DOP-PCR was confirmed by the analysis of 152 copy number changes in ten tumour samples. We assume that one of the most distorting e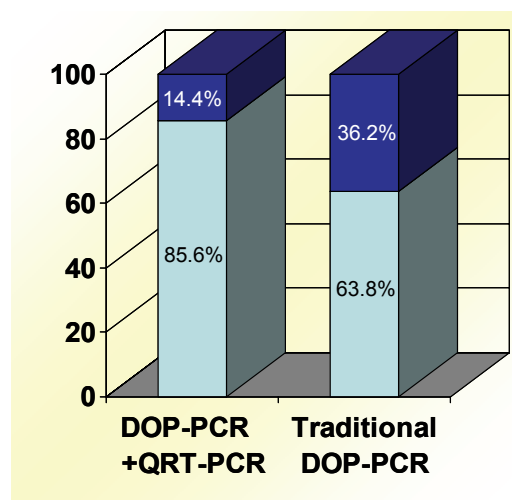ffects of the DOP-PCR technique in the study of amplified genomic DNA is the over-amplification of the products. Over-amplification has a dramatic distorting effect on the original genomic rearrangements and can generate false result. This effect can be decreased by adding QRT-PCR to the original protocol. Since DOP-PCR is a widely used technique and the preservation of the original genome set is especially important in genomic studies, therefore we propose to include QRT-PCR to follow and control the amplification status.

7.2. A second field metachronous MCC of the lip and the palatine tonsil

MCCs are highly divergent when analysed for chromosome aberrations (84, 86, 87). Reported recurrent chromosomal imbalances detected by CGH analysis were loss of 3p, 10q, 13q and 17p and gains of 1q, 3q, 5p and 8q (87). In the present study, we could also detect the loss of 3p and 17p, but none of the above-mentioned amplified regions could be confirmed (Table 4, Figure 6).

Table 4. Common and individual gains and losses of MCC and the tonsillar tumour detected by CGH.

	Deletion	**Amplification**
both tumour	1p36, 1p31, 1p13, 1q21-23, 1q32, 1q42.13, 2p13, 2p11.2, 2q35, 3p21, 3q13.2, 3q14.3, 3q26-28, 4p16, 4q21, 5q35, 6p21, 6q24, 7q21, 8p21, 8q24, 9p12, 9q34, 11p11.2, 11q13, 11q23.3, 12q24.1, 14q11.2, 15q23-24, 16p13-12, 16q24, 17p13, 17q12, 17q23, 18q12, 18q21, 19p13, 20p13, 21q22, 22q13.1, X monosomy	2p23, 10p15
Merkel cell carcinoma	11p11.2, 11q12.3, 12q13, 16p13.1, 17q21.1, 17q25	2p25, 12q12, 15q14
mesopharynx	1p34.1-32.2, 1p21-22, 1q42, 2q37, 4p16.3, 4q28.3, 5q11.1, 5q22, 5q31-32, 7p14, 8p22-24.13, 10q21.1, 11pter-p15.5, 12q14.3, 14q11.2, 14q31-32, 15q11-13, 16q23-24, 17q21.3-q23, 20q13.1, 21q22.13, 22q11	–

In another study, only 3 of the 10 MCCs exhibited common gains and losses and they shared a gain of 8q21-q22 and a loss of 4p15-pter (86). In the present study, the 4p16 region was also found to be deleted in both the primary and secondary tumours. Unfortunately, to date no known tumour suppressor gene has been mapped to this region (Table 5). Speleman's

group detected losses involving the entire chromosome 10 or partial loss of the chromosome 10 long arm in one-third of the MCC cases they analysed with a possible loss of heterozygosity (LOH) of 10q23, including the PTEN tumour-suppressor gene (85). In our case, deletion of this region was not observed in either tumour sample.
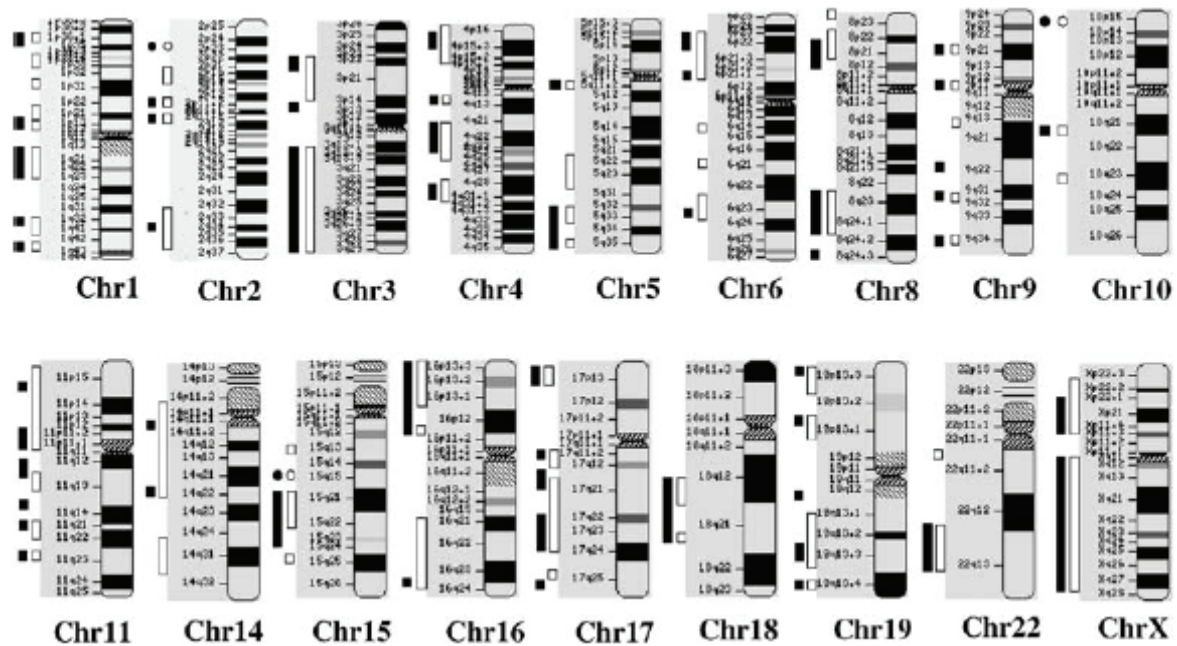
Figure 6. Copy number aberrations found using microarray CGH analysis and real-time polymerase chain reaction of primary MCC and the tonsillar cancer. Boxes on the left side of each chromosome ideogram show regions of reduced copy number (losses of DNA in the tumour genome). Circles on the left side of each chromosome ideogram show regions of increased copy number (gains of DNA in the tumour genome). Filled boxes denote MCC and empty boxes tonsillar tumour

In previous observations, series of MCCs showed no evidence of high-level amplification (87). Recurrent gains of chromosomes 1, 6, 18q and 20 were detected in 2 cases (84). In our case, only 2 regions, 2p and 10p were commonly over-represented. In a very recent study, 19 primary MCCs were analysed by CGH and in 13 samples extensive gains and losses were detected (155). It was shown that a majority of the alterations were gains, while only a few common losses were detected, mainly in regions 4q, 13q and 16q. Neither of our gains was found in any of the 19 cases they analysed. Most of the losses were detected in at least one case reported in the above-mentioned study, but the 13 MCCs exhibited a very heterogenous pattern, with diverse regions with losses.

Our CGH results revealed several new and a few other previously known chromosomal regions that have been presumed to be involved in the pathogenesis of MCC. We found 2 common gains and 41 common losses in the 2 samples. However, in 31 chormosome locations we observed differences in gene copy numbers between the 2 tumours. From the results obtained by CGH analysis, we believe that the mesopharynx cancer and the MCC of the lip derived from the same, genetically altered field, thus the mesopharynx cancer can be regarded as a second field tumour. From the results obtained by CGH analysis, we hypothesize that Merkel cells in two adjacent anatomical sites, i.e. in the lip and mesopharynx, underwent same precancerous genetic alteration, and both tumours arose from a common cell clone. If our hypothesis is correct, the mesopharynx cancer can be regarded as a second field tumour.

Table 5. Apoptotic genes and tumour supressors mapped to regions with common chromosomal aberrations. (Apoptotic and tumour suppressor genes in bold character. Apoptotic and tumour suppressor related genes in italics in brackets.)

Chromosome location	Apoptotic genes	Tumour suppressors	Chromosome location	Apoptotic genes	Tumour suppressors
In both tumour					
1p36	**DFFB, TP73, CASP9** *(CDC42, MFN2)*	**UBE4B, TUSC3, PRDM2, C1orf1, ALPL** *(E2F2, TP73)*	11p11.2	*(MADD)*	
1p31	_	**CLCA2**	11q13	**DPF2, BAD, FADD** *(RELA, CCND1, RAD9A)*	**DOC-1R, MEN1** *(ST3, CCND1, SHANK2)*
1p13	_	**ST7L**	11q23.3		**THY1**
1q21-23	**MCL1, DAP3, TNFSF6** *(MUC1, APCS, CRP, SELL)*		12q24.1	*(SCA2)*	
			16p13-12	**ASC**	**TSC2**
2p13		**MAD**	16q24		**WFDC1, GAS8, MGC15419, CBFA2T3**
3p21.3	*(CCR3)*	**RASSF1, BAP1** *(SEMA3B)*	17p13		***TP53, HIC1, OVCA2, DPH2L1***
3q26-28	*(ETV5, OPA1)*	**TSBF1**	17q12	*(CCR7)*	*(MPP3)*
4p16		*(GAK)*	18q21	*(BCL2)*	**DCC, SERPINB5** *(E2F5)*
4q21	*(SNCA)*				
5q35		*(PDLIM7)*	19p13		**DIRAS1** *(TJP3, SMARCA4, GIPC3)*
6p21	**BAK1, TNF** *(HSPA)*	*(CDKN1A)*			
6q24		**SASH1** *(PLAGL1)*	21q22	*(MX1)*	
8p21	**BNIP3** *(CLU)*	***PDGFRL*** *(CNOT7, PDLIM2)*	22q13.1	*(HMOX1)*	**ST13**
			Xp22.1	*(SH3KBP1)*	
8q24		*(RNF139)*	Xq12		**ING2**
9q34	**TRAF2** *(ABL1)*		Xq28		**RPL10**

Several oncogenes and tumour-suppressor and apoptotic genes were assumed to be changed in their copy number, and many of them were mapped to the regions having changes in their copy number in one or both of the tumours (Tables 5 and 6).

Table 6. Apoptotic genes and tumour supressors mapped to regions with chromosomal aberrations specific to MCC or tonsillar tumour.

Chromosome location	Apoptotic genes	Tumour suppressors
In Merkel cell carcinoma		
11p11.2	*(MADD)*	
12q13	*(CDK2, KRT18, NR4A1, WNT1)*	
17q25	**BIRC5**	
In Mesopharynx		
1p34.1-32.2		**FABP3**
3p22-21		**ADPRTL3**
5q11.1	*(LOC145908)*	
5q22		**MCC**
5q31-32		**C5orf7**
10q21.1	*(CDC2)*	
11pter-p15.5	*(CTSD, HRAS)*	**MRVI1**
14q31-32	**SIVA**	
16q23-24	*(LOC145908)*	**CBFA2T3**
21q22.13		**RUNX1**
22q11	**BID**	**MYO18B**

The limitation of this list is that in these cases the deletions of the genes themselves were not proven in this study; only those regions were determined which were located to certain regions or proximity to regions where DNA segments on the microarrays originated.

The micorarray-based CGH techniques used in this study could result in distorted data, especially when paraffin-embedded tissue is the target. Another limitation of this study is that the deleted regions were determined by using hybridizations based on complementary cDNA - genomic DNA annealing events, which could generate more biases. As a consequence of the above problems, we determined the reliability of the results obtained by the CGH microarray by using QRT-PCR. 10 genes were selected to follow the copy number changes by QRT-PCR. Out of the 10 genes, one exhibited no changes in the copy number found by CGH microarray analysis in all cases: the dihydrofolate reductase gene. This was therefore used an internal control. The copy numbers of all the other 9 genes (sequences and chromosome locations are listed in Table 2, accesion numbers are listed in Table 7) were related to this inner control. We used DNA purified from normal lymphoid tissue as control and determined copy number changes of the other two tumours (Table 4, Figure 6).

We confirmed the deletions in 7 cases for both tumours and 2 were confirmed for only MCC. Although the number of the confirmatory QRT-PCRs were limited and therefore does not allow determination of the reliability of the CGH methods, the main purpose of the study

was to determine the relation of the two tumours, not a precise determination of the deleted regions.

Table 7. Confirmation of CGH data by QRT-PCR. Only two common losses could not be confirmed. Gains are indicated as grey background.

Microarray data confirmed by QPCR	Clone name	Accesion No.	Chrom. location	Distance
both tumour	Steroid 5-alpha-reductase 2 (SRD5A2)	M74047	2p23	31724
	Hepatocyte nuclear factor-3 alpha	U39840	14q12-q13	36052
	Zinc finger protein	AF020591	19q13.43	63450
	Androgen receptor (dihydrotestosterone receptor)	M23263	Xq12	63075
	C8FW phosphoprotein	AJ000480	8q24.13	126404
	ESTs, Highly similar to Phosohatidylcholine transfer protein	AA933627	17q23	54340
	Cytochrome P450, subfamily XIA	M14565	15q23-24	70670
Merkel cell carcinoma	EST	N22765	15q14	no data
	Cardiac myosin binding protein-C	U91629	11p11.2	49310

We confirmed the deletions in 7 cases for both tumours and 2 were confirmed for only MCC. Although the number of the confirmatory QRT-PCRs were limited and therefore does not allow determine the reliability of the CGH methods, the main purpose of the study was to determine the relation of the two tumours, not a precise determination of the deleted regions.

In summary, the partly different molecular patterns obtained by CGH, the similar histological features, and the close proximity to the primary tumour indicate that the tonsillar cancer was a second field tumour. The common origin was further confirmed, because out of 3 early markers (9p, 3p and 17p) two of them (9p and 17p) were common in both cancer samples, one (17p) bearing the p53 tumour suppressor marker gene. The common copy number changes do not support the possibility that the tonsillar cancer was a second primary tumour. The tonsils are very rare and unusual sites of metastatic disease in MCC. There are three reports in the literature describing oropharyngeal metastasis of a MCC (71, 156, 157). In all these reports, the metastasis occurred within 24 months after resection of the primary tumour. In our case, it was clinically very unlikely that the tonsillar tumour was a metastasis of the MCC of the lip, because no local recurrence or regional lymph node metastasis or distant haematogenous metastases were observed in the 7-year follow-up. In harmony with

the clinical situation, the molecular patterns of the 2 tumours were not similar, therefore the possibility of a metastasis could be rejected. Although the concept of second primary tumours and field cancerization has been formulated for oral and oropharyngeal squamous cell carcinomas (78), our results indicate that Merkel cells in adjacent anatomic sites may also be the targets of field cancerization.

7.3. Determination of several copy number changes in different genomic DNA of thyroid carcinoma based on disease course

We obtained genomic DNA from paraffin-embedded samples of primary- and terminal-stage APTC of a sixty-three-year-old male patient (by the latter, histology indicated dedifferentiation), which genomic DNA was amplified by our improved DOP-PCR technique. As a follow-up, relative DNA losses and gains were determined for each tumour sample by normalizing the intensities to the values obtained after hybridization with labeled probes from GPTC. The CGH-array analysis were performed on human cDNA microarray containing 3200 gene-specific cDNA samples in duplicate on glass slides.

Specific primers were designed for thirty chromosomal regions exhibiting changes (deletion or amplification) in order to confirm our CGH results using QRT-PCR, which was performed on the original, non-amplified genomic DNA. We found that 3 out of the 30 regions (FGF7, EIF4EBP3, KIAA0549) indicated the same changes (DNA losses) in both tumours and corresponded to CGH-array results. In one case (Image EST-Acc. No. R78712), the QRT-PCR results corresponded to the CGH-array data of primary APTC; and at further examination, DNA gain was detected in the case of terminal-stage APTC when it was compared to the copy number of normal thyroid tissue. These results demonstrated a difference in chromosome copy numbers of primary and terminal-stage APTC.

Further on, two additional gene loci were identified with changes only within terminal-stage APTC, namely Tre-2 oncogene and TB10, which were positive in each thyroid carcinoma during immunohistochemical experiments – especially in the case of ATC (158). Only one region – Tre-2 oncogene – out of six regions was confirmed as over-represented in the case of GPTC.

Thirty two additional thyroid carcinomas examined as well. QRT-PCR analysis was performed on the non-amplified genomic DNA of 32 PTCs as well as the first GPTC and the first terminal-stage APTC, upon which the CGH-array analysis was carried out. The copy

number of the six regions described above (Table 8) was determined on 34 thyroid carcinoma genomes altogether (10 GPTCs; 14 IPTCs, 10 APTCs); we compared it with two normal thyroid samples, and the relative ratios were normalized to the copy numbers of the alpha1-fetoprotein transcription factor and the H3 histone (family 3A) as internal control genes separately.

Since we could not detect a significant difference in the examined six regions – in the copy numbers of IPTC and APTC samples, these two groups were treated as one group (I/APTC) (that is where the patient had a lymph node metastasis in the cervical areas or some other distant metastasis /spread: lung, bone/, suffered from local recurrance, died because of their PTC).

Table 8. Copy number alterations in different disease course thyroid carcinoma. Dark gray denotes DNA gains common amplification of TB10 and Image EST, while light gray denotes separately amplification.

Gene	Thymosin, beta 10		Image EST Acc.No.R78712		Tre-2 oncogene		KIAA0549 protein		Fibroblast growth factor 7		EIF4EBP3	
Chrom. Loc.	5q31.3		15q25		17p13		2q33		15q15-q21.1		5q31.3	
	Mean (SD)		Mean (SD)		Mean (SD)		Mean (SD)		Mean (SD)		Mean (SD)	
GPTCs ('A' group)	1.35 (0.20)	N	3.28 (1.93)	A	0.75 (0.07)	N	0.58 (0.26)	N	0.99 (0,10)	N	0.39 (0.16)	D
	1.31 (0.32)	N	1.26 (0.32)	N	2.62 (0.88)	N	0.59 (0.19)	N	0.86 (0.35)	N	0.53 (0.15)	D
	1.29 (0.17)	N	0.46 (0.15)	D	1.80 (0.31)	A	0.54 (0.13)	D	0,74 (0.18)	N	0.31 (0.06)	D
	1.12 (0.41)	N	0.49 (0.25)	D	2.63 (1.14)	A	0.46 (0.18)	D	0.52 (0.16)	D	0.35 (0.10)	D
	1.14 (0.30)	N	0.98 (0.34)	N	1.64 (0.28)	A	1.10 (0.25)	N	1.13 (0.24)	N	0.69 (0.23)	N
	0.95 (0.27)	N	0.67 (0.26)	N	2.74 (0.80)	A	0.58 (0.22)	N	0.45 (0.05)	D	0.89 (0.39)	N
	1.88 (0.13)	A	1.27 (0.34)	N	3.14 (0.95)	A	0,00	D	1.11 (0.10)	N	0.52 (0.08)	D
	1.18 (0.35)	N	0.64 (0.56)	N	2.24 (0.83)	A	0.48 (0.04)	D	0.91 (0.31)	N	0.40 (0.35)	D
	0.70 (0.22)	N	0.89 (0.22)	N	0.69 (0.64)	N	0,09 (0.07)	D	1.65 (0.27)	A	0.18 (0.07)	D
	2.96 (1.18)	A	0.81 (0.29)	N	2.19 (0.12)	A	0.64 (0.36)	N	0.97 (0.32)	N	1.20 (0.43)	N
IPTCs ('B' group)	2.95 (1.10)	A	0.90 (0.32)	N	1.28 (0.46)	N	0.52 (0.26)	D	0.49 (0.15)	D	0.63 (0.15)	N
	2.02 (0.60)	A	0.70 (0.34)	N	3.82 (0.30)	A	0.36 (0.09)	D	0,47 (0.23)	D	0.64 (0.23)	N
	1.79 (0.63)	A	0.54 (0.28)	D	3.99 (1.16)	A	0.40 (0.21)	D	0.49 (0.23)	D	0.55 (0.26)	D
	3.03 (0.99)	A	2,36 (0.94)	A	1.51 (0.37)	A	1.33 (0.26)	N	0.65 (0.16)	N	0.79 (0.23)	N
	1.13 (0.29)	N	0.66 (0.18)	N	3.93 (1.96)	A	0.39 (0.09)	D	0.40 (0.14)	D	0.20 (0.06)	D
	0.83 (0.13)	N	3.64 (1.64)	A	2.82 (0.17)	N	1.06 (0.26)	N	5.26 (0.54)	A	1.14 (0.33)	N
	0.92 (0.41)	N	1.09 (0.41)	N	1.26 (0.21)	N	0.82 (0.25)	N	1.03 (0.21)	N	0.79 (0.26)	N
	4.87 (1.08)	A	2.38 (1.07)	A	5.00 (1.51)	A	1.08 (0.19)	N	8.14 (0.84)	A	0.85 (0.31)	N
	4.27 (1.19)	A	1.86 (0.97)	A	2.33 (0.72)	A	1.14 (0.35)	N	1.16 (0.12)	N	0.37 (0.10)	D
	1.32 (0.29)	N	1.30 (0.73)	N	3.24 (0.84)	A	2.03 (0.54)	A	1.18 (0.28)	N	0.73 (0.17)	N
	1.67 (0.34)	A	2.25 (1.27)	A	1.73 (0.43)	A	3.39 (1.04)	A	1.90 (0.39)	A	1.10 (0.29)	N
	1.02 (0.13)	N	1.12 (0.46)	N	1.97 (0.52)	A	0.72 (0.17)	N	1.18 (0.27)	N	0.81 (0.16)	N
	4.13 (1.85)	A	0.67 (0.20)	N	3.67 (0.50)	A	0.25 (0.12)	D	1.47 (0.18)	N	0.42 (0.14)	D
	2.00 (0.56)	A	0.93 (0.29)	N	3.92 (1.14)	A	0,00	D	0.72 (0.07)	N	0.58 (0.20)	N
APTCs ('B' group)	3.77 (1.25)	A	0.53 (0.21)	D	3.46 (1.59)	A	0.65 (0.21)	N	0.37 (0.22)	D	0.69 (0.26)	N
	4.16 (1.19)	A	0.53 (0.28)	D	2.29 (0.69)	A	0.21 (0.11)	D	0.66 (0.36)	N	0.21 (0.06)	D
	0.72 (0.13)	N	0.68 (0.22)	N	0.91 (0.18)	N	0.38 (0.15)	D	0.62 (0.19)	N	0.51 (0.19)	D
	3.27 (0.79)	A	0.84 (0.40)	N	2.95 (0.60)	A	0.06 (0.04)	D	0,.76 (0.30)	N	0.28 (0.10)	D
	1.50 (0.34)	A	0.72 (0.19)	N	1.15 (0.32)	N	0.46 (0.20)	D	0.83 (0.42)	N	0.35 (0.11)	D
	1.35 (0.34)	N	0.53 (0.20)	D	4.47 (1.65)	A	0.58 (0.23)	N	0.50 (0.18)	D	0.70 (0.27)	N
	2.07 (0.66)	A	2.11 (0.66)	A	1,15 (0.41)	N	0.76 (0.15)	N	0.85 (0.32)	N	0.65 (0.20)	N
	0.77 (0.18)	N	7.34 (6.65)	A	3.52 (0.90)	A	0.71 (0.24)	N	2.95 (1.84)	A	0.78 (0.22)	N
	0.80 (0.15)	N	0.71 (0.31)	N	1.75 (0.25)	A	1.91 (0.52)	A	0.97 (0.17)	N	1.18 (0.35)	N
	3.32 (2.52)	A	2.06 (1.86)	A	2.44 (2.10)	A	0.26 (0.37)	D	0.50 (0.43)	D	0.62 (0.30)	N

In the present study, Tre-2 oncogene was found to be over-represented in 80% of the GPTC and I/APTC groups (Figure 7). Tre-2 is a recombinant gene isolated from NIH3T3 cells transfected with human Ewing's sarcoma DNA. Genetic elements of Tre-2 originate from chromosomes 5, 18 and 17. Our examined field of Tre-2 oncogene is mapped onto the 17p13 chromosome region. Many researchers have demonstrated that this oncogene is consistently transcribed in various human cancer cells (159). Expression of Tre-2 in normal somatic cells, however, has not yet been reported. Tre-2 oncogene seems to encode a nonfunctional Rab (GAP). Regions flanking the TBC (Tre-2/Bub2/Cdc16) domain may be crucial for catalytic activity. These domains are predicted to encode GTPase-activating proteins (GAPs) for Rab family G proteins. Martinu et al. (160) have identified this oncogene as a novel regulator of the Arf6-regulated plasma membrane recycling system. Masuda-Robens et al. have demonstrated that Tre-2 coprecipitated specifically with the active forms of Cdc42 and Rac1 in vivo, which play fundamental roles in transformation and actin remodeling.
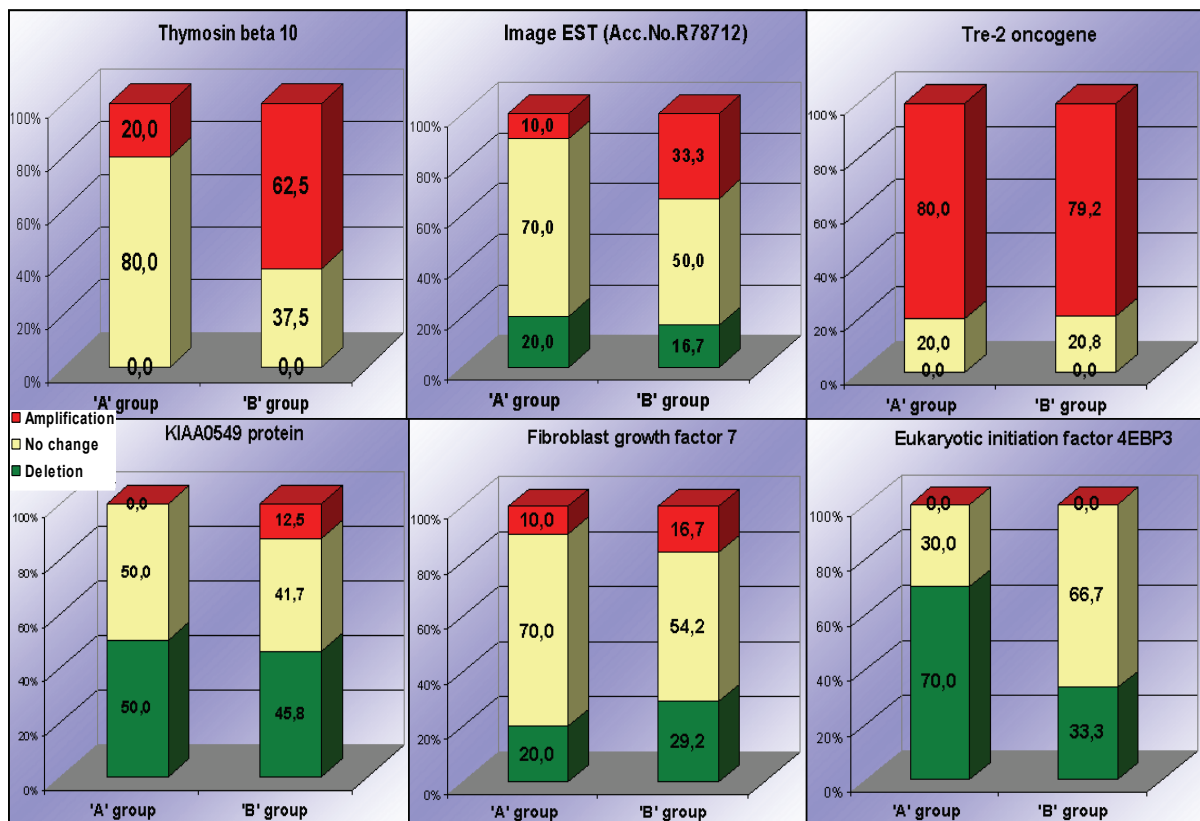

Figure 7. Copy number alterations of six chromosomal regions in two disease course thyroid carcinomas.
('A' group: PTC of good disease outcome; 'B' group: intermediate and aggressive type of PTC)

Our study showed amplified regions of TB10 in greater extent in I/APTC (62.5%), whereas in the case of GPTC group the quantity of DNA gains could be detected in only 20% of the cases. This is a significant difference between the two groups based on the outcome of the disease. Chiappetta et al. (161) have shown that TB10 gene expression can function as a possible tool in the diagnosis of thyroid neoplasias, since TB10 positive staining was found in all human thyroid carcinoma, particularly in the anaplastic histotypes. Many researchers have demonstrated that TB10 acts as an actin-mediated tumour suppressor (162). Some observations suggest that TB10 plays a significant role in the cellular processes controlling apoptosis (163). Other authors have shown that the TB10 gene is highly expressed in human thyroid carcinoma cell lines and tissues, whereas its expression is almost undetectable in normal thyroid; furthermore, TB10 gene expression can function as a useful marker for diagnosis and prognosis of a large variety of human cancers (162). In a study by Takano et al. (158), TB10 mRNA is highly over-expressed in human and experimental thyroid tumours and its expression is abundant in undifferentiated thyroid carcinomas (158, 164). These results seem to be closely related to our results in connection with genomic rearrangement. TB10 gene overexpression is a general event in human carcinogenesis (162). Overexpression of TB10 was showed in thyroid, pancreatic, gastric, breast, ovarian, uterine, colon, esophageal cancer and germ cell tumours. Lee et al. (165) have described that overexpressed TB10 significantly inhibited vascular endothelial growth factor-induced endothelial cell proliferation, migration, invasion and tube formation *in vitro*.

The examined Image EST (Acc. No. R78712) is mapped to the middle of the AKAP13 gene. In the case of this region, our results indicated DNA gains in one case of the GPTC group and in an ascending quantity in the I/APTC. We can postulate that the AKAP13 gene is affected; however, further analysis is needed to provide this hypothesis. AKAP13 anchors both protein kinase A and 14-3-3, and by this means inhibits the Rho-GEF activity of the AKAP-Lbc signaling complex (166). Alternative splicing of this gene results in at least 3 transcript variants encoding different isoforms containing a dbl oncogene homology (DH) domain and a pleckstrin homology (PH) domain. The DH domain is associated with guanine nucleotide exchange activation for the Rho/Rac family of small GTP binding proteins, resulting in the conversion of the inactive GTPase to the active form capable of transducing signals.

In two regions we found DNA losses, in one case out of which – the EIF4EBP3 gene – indicated a decreased copy number in many cases during our experiments. This protein is the negative regulator of protein byosinthesis and the initiation of translation; in other words, it represses translation. DNA losses were detected in 70% of the GPTC and only in 33% of I/APTC. The KIAA0549 gene was under-represented in half of both groups. When examined, the sixth gene, namely FGF7, demonstrated both DNA gains and losses in small quantity, but this rearrangment was greater in the case of I/APTC. FGF family members possess broad mitogenic and cell survival activities, and are involved in a variety of biological processes, including embryonic development, cell growth, morphogenesis, tissue repair, tumour growth and invasion. Unfortunately, we do not have knowledge on the role these rearrangements of genes can play within the tumourigenesis progress.

Our results indicate that synchronous detection of over-representation of TB10 and Image EST (Acc. No. R78712) can become a good diagnostic marker for aggressive thyroid carcinoma.

7.4. QRT-PCR-based exponential amplification for microarray gene expression profiling

Global RNA expression analysis using microarray technology allows the identification of genes that are differentially expressed in tumour versus normal tissues. In this case the elimination of overamplified cDNA is also extremely important, for this reason we developed an alternative exponential sample amplification method. Total RNA was reverse transcribed and amplified with two PCR protocols resulting in DNA samples from early phase (13th–15th cycles) and late exponential, early saturation phase (21st cycle), similarly to the proving of the reliability of the improved DOP-PCR, which can amplify the whole genome. Reproducibility and reliability of the methods were determined performing cDNA microarray and confirmative QRT-PCR experiments on LPS-treated mouse macrophage cDNA prepared in a different manner.

Our exponential sample amplification protocol preserves the original expression ratios and allows unbiased gene expression analysis from minute amounts of starting material.

7.5. Analysis of the gene expression pattern of parallel expression of αIIbβ3 and αvβ3 integrins in human melanoma cells using microarray technology

In cancerous tissues new vessels are required to provide cancer cells with nutrients and are targets for invading cancer cells themselves. At the beginning of its natural history, a cancer is not vascularised, and it does not grow beyond 2 mm in size unless vascularisation has occurred. The switch to the angiogenic phenotype is a critical point in tumour progression (167) and depends on the additive effect of progressive genetic alterations (168).

The effect of αIIbβ3-transfection on gene expression was tested using a homemade 3200 cDNA microarray (43, 150). The fastest growing and most vascularized clone (19H) was selected and compared to the mock cells, 3.1P to reveal the molecular pathomechanism of large growth and cell survival. We defined those genes to be regulated by αIIbβ3 transfection in melanoma cell cultures, in the case of which the average-fold change (increase or decrease) of the 4 data points was at least 2.0-fold.

Forty-eight genes in 19H cells corresponded to such strict criteria from the 3200 analysed; 36 genes were found to be upregulated and 12 have been downregulated. Among the downregulated genes, there were no known angiogenic/endothelial ones represented; however, among the 19 known genes upregulated in 19H cells compared to 3.1P, 3 could be considered endothelial-specific, such as CD34 antigen, endothelin receptor type B and prostaglandin I-2 synthase, the changes of which were also confirmed by QRT-PCR analysis (data not shown).

Parallel expression of the two β3-integrins in human melanoma cells induced modulation not only of bFGF but of other genes as well, which is demonstrated by microarray analysis. Interestingly, 3 out of 19 known genes upregulated significantly in αIIbβ3-transfected 19H cells are endothelial cell-specific genes, CD34, endothelin receptor B and prostaglandin I-2 synthase. Recapitulation of an embryonic endothelial/angioblastic genetic program, called vasculogenic mimicry (169), resulting in vivo formation of tumour cell lined vascular channels, was recently described and documented in case of human melanoma and other tumours (170). There have been several genes identified to be responsible for this vasculogenic phenotype including VE-cadherin, CD34, TIE2, EphA2, LAMC2, endoglin, EDG1, ESM1 and EDF1 (171).

VIII. CONCLUSIONS

In many cases only a minute amount of partially degraded genomic DNA can be extracted from archived clinical samples. Forensic analyses, tests on biopsy samples, prenatal diagnosis and many other investigations have access to very little starting material. Investigations of the genetic background of intratumour heterogenity require manipulation of minute amounts of neoplastic tissue on a cellular scale, often below the amounts required for routine CGH. A method to overcome the small quantity of the DNA available is to perform whole genome amplification. One commonly used method is DOP-PCR, due to its simplicity and degree of success. In our study a new QRT-PCR-based DOP-PCR amplification method was developed, on the basis of which we have proved the preservation of the original copy number of different chromosomal regions in amplified genomic DNA.

This improved genomic amplification technique was also applied in the case of two clinical investigations, during which the molecular imbalances of tumours were detected by microarray based CGH analysis. In the first case we analysed the MCC and the seven years later appearing tonsillar tumour in order to assess the genetic relationship of the tumours. On the basis of our results we have demonstrated that the tonsillar tumour can be pathogenetically regarded as a second field tumour.

The improved DOP-PCR technique was also employed for detection of molecular patterns of PTCs of different disease courses. The question arises as to whether genomic differences (markers) are to be found at the appearance of the disease, or an unfavorable outcome can be predicted that could allow a more effective treatment for the patient. Our CGH-array and QRT-PCR results have shown rearrangements of six regions of the genome, which can play a role in the tumourigenesis progress, and synchronous detection of some of these genes can become a good diagnostic marker for the detection of malignant thyroid carcinoma.

After reaching a certain tumour size, tumour cells need to be provided with a sufficient amount of oxygen and nutriment. It was demonstrated that the transfection of integrin $\alpha IIb\beta 3$ into human melanoma cells promoted their *in vivo* growth and cell survival. We have revealed nineteen known genes upregulated in transfected melanoma cells; three could be considered endothelial-specific by performing microarray experiments, which can provide explanation for a part of underlying pathomechanism of increased cancer growth and angiogenesis.

IX. ACKNOWLEDGMENTS

X. REFERENCES

1. Pardue ML, Gall JG. Molecular hybridization of radioactive DNA to the DNA of cytological preparations. *Proc Natl Acad Sci U S A*. 1969;64:600-4.
2. John HA, Birnstiel ML, Jones KW. RNA-DNA hybrids at the cytological level. *Nature*. 1969; 223:582-7.
3. Schrock E, du Manoir S, Veldman T, et al. Multicolor spectral karyotyping of human chromosomes. *Science*. 1996; 273:494-7.
4. Kallioniemi A, Kallioniemi OP, Sudar D, et al. Comparative genomic hybridization for molecular cytogenetic analysis of solid tumours. *Science*. 1992; 258:818-21.
5. Abeln EC, van Kemenade FD, van Krieken JH, et al. Rapid identification of mixed up bladder biopsy specimens using polymorphic microsatellite markers. *Diagn. Mol. Pathol*. 1995; 4:286–91.
6. Orita M, Iwahana H, Kanazawa H, et al. Detection of polymorphisms of human DNA by gel electrophoresis as single-strand conformation polymorphisms. *Proc Natl Acad Sci U S A*. 1989; 86:2766-70.
7. Myers RM, Maniatis T, Lerman LS. Detection and localization of single base changes by denaturing gradient gel electrophoresis. *Methods Enzymol*. 1987; 155:501-27.
8. Dracopoli, N.C. Ed. "Detection of Mutations by RNase Cleavage". Current Protocols in Human Genetics. 1998. John Wiley & Sons, Inc.
9. Roest PA, Roberts RG, Sugino S, et al. Protein truncation test (PTT) for rapid detection of translation-terminating mutations. *Hum Mol Genet*. 1993; 2:1719-21.
10. Maxam AM, Gilbert W. A new method for sequencing DNA. 1977. *Biotechnology*. 1992; 24:99-103.
11. Frommer M, McDonald LE, Millar DS, et al. A genomic sequencing protocol that yields a positive display of 5-methylcytosine residues in individual DNA strands. *Proc Natl Acad Sci U S A*. 1992; 89:1827-31.
12. Greider CW, Blackburn EH. Telomeres, telomerase and cancer. *Sci. Am*. 1996; 276:92–97.
13. Chuang SE, Daniels DL, Blattner FR. Global regulation of gene expression in Escherichia coli. *J Bacteriol*. 1993; 175:2026-36.
14. DeRisi JL, Iyer VR, Brown PO. Exploring the metabolic and genetic control of gene expression on a genomic scale. *Science*. 1997; 278:680-6.
15. Nelson SF, McCusker JH, Sander MA, et al. Genomic mismatch scanning: a new approach to genetic linkage mapping. *Nat Genet*. 1993; 4:11-8.
16. Haab BB, Dunham MJ, Brown PO. Protein microarrays for highly parallel detection and quantitation of specific proteins and antibodies in complex solutions. *Genome Biol* 2001;. 2, RESEARCH0004.
17. Zhu H, Klemic JF, Chang S, Bertone P, et al. Analysis of yeast protein kinases using protein chips. *Nat Genet*. 2000; 26:283-9.
18. Ziauddin J, Sabatini DM. Microarrays of cells expressing defined cDNAs. *Nature*. 2001; 411:107-10.
19. Kuruvilla FG, Shamji AF, Sternson SM, et al. Dissecting glucose signalling with diversity-oriented synthesis and small-molecule microarrays. *Nature*. 2002; 416:653-7.
20. Schena M, Shalon D, Davis RW, et al. Quantitative monitoring of gene expression patterns with a complementary DNA microarray. *Science*. 1995; 270:467-70.
21. Zvara A, Hackler LJr, Nagy ZB, et al. New molecular methods for classification, diagnosis and therapy prediction of hematological malignancies. *Pathol Oncol Res*. 2002; 8:231-40.

22. Jenson SD, Robetorye RS, Bohling SD, et al. Validation of cDNA microarray gene expression data obtained from linearly amplified RNA. *Mol Pathol*. 2003; 56:307-12.

23. Saksela K, Stevens C, Rubinstein P, et al. Human immunodeficiency virus type 1 mRNA expression in peripheral blood cells predicts disease progression independently of the numbers of CD4+ lymphocytes. *Proc Natl Acad Sci U S A*. 1994; 91:1104-8.

24. Futscher BW, Blake LL, Gerlach JH, et al. Quantitative polymerase chain reaction analysis of mdr1 mRNA in multiple myeloma cell lines and clinical specimens. *Anal Biochem*. 1993; 213:414-21.

25. White TJ, Madej R, Persing DH. The polymerase chain reaction: clinical applications. *Adv Clin Chem*. 1992; 29:161-96.

26. Wackym PA, Simpson TA, Gantz BJ, et al. Polymerase chain reaction amplification of DNA from archival celloidin-embedded human temporal bone sections. *Laryngoscope*. 1993; 103:583-8.

27. O'Garra A, Vieira P. Polymerase chain reaction for detection of cytokine gene expression. *Curr Opin Immunol*. 1992; 4:211-5.

28. Kittler R, Stoneking M, Kayser M. A whole genome amplification method to generate long fragments from low quantities of genomic DNA. *Anal Biochem*. 2002; 300:237-44.

29. Barbaux S, Poirier O, Cambien F. Use of degenerate oligonucleotide primed PCR (DOP-PCR) for the genotyping of low-concentration DNA samples. *J Mol Med*. 2001; 79:329-32.

30. Simpson DJ, Bicknell EJ, Buch HN, et al. Genome-wide amplification and allelotyping of sporadic pituitary adenomas identify novel regions of genetic loss. *Genes Chromosomes Cancer*. 2003; 37:225-36.

31. Klein CA, Schmidt-Kittler O, Schardt JA, et al. Comparative genomic hybridization, loss of heterozygosity, and DNA sequence analysis of single cells. *Proc Natl Acad Sci U S A;*1999; 96:4494-9.

32. Ludecke HJ, Senger G, Claussen U, et al. Cloning defined regions of the human genome by microdissection of banded chromosomes and enzymatic amplification. *Nature*. 1999; 338:348-50.

33. Saunders RD, Glover DM, Ashburner M, et al. PCR amplification of DNA microdissected from a single polytene chromosome band: a comparison with conventional microcloning. *Nucleic Acids Res*. 1989; 17:9027-37.

34. Zhang L, Cui X, Schmitt K, et al. Whole genome amplification from a single cell: implications for genetic analysis. *Proc Natl Acad Sci U S A*. 1992; 89:5847-51.

35. Dietmaier W, Hartmann A, Wallinger S, et al. Multiple mutation analyses in single tumour cells with improved whole genome amplification. *Am J Pathol*. 1999. 154:83-95.

36. Telenius H, Carter NP, Bebb CE, et al. Degenerate oligonucleotide-primed PCR: general amplification of target DNA by a single degenerate primer. *Genomics*. 1992; 13:718-25.

37. Nagy J, Feher LZ, Sonkodi I, et al. A second field metachronous Merkel cell carcinoma of the lip and the palatine tonsil confirmed by microarray-based comparative genomic hybridisation. *Virchows Arch*. 2005; 446:278-86.

38. Nelson DL,. Ledbetter SA, Corbo L, et al. Alu polymerase chain reaction: a method for rapid isolation of human-specific sequences from complex DNA sources. *Proc Natl Acad Sci U S A*. 1989; 86:6686-90.

39. Dean FB, Hosono S, Fang L, et al. Comprehensive human genome amplification using multiple displacement amplification. *Proc Natl Acad Sci U S A*. 2002; 99:5261-6.

40. Phillips J, Eberwine JH. Antisense RNA Amplification: A Linear Amplification Method for Analyzing the mRNA Population from Single Living Cells. *Methods*. 1996; 10:283-8.

41. Dean FB, Nelson JR, Giesler TL, et al. Rapid amplification of plasmid and phage DNA using Phi 29 DNA polymerase and multiply-primed rolling circle amplification. *Genome Res*. 2001; 11:1095-9.

42. Lizardi PM, Huang X, Zhu Z, et al. Mutation detection and single-molecule counting using isothermal rolling-circle amplification. *Nat Genet*. 1998; 19:225-32.

43. Puskas LG, Zvara A, Hackler L Jr, et al. RNA amplification results in reproducible microarray data with slight ratio bias. *Biotechniques*. 2002; 32:1330-40.

44. Puskas LG, Fartmann B, Bottka S. Restricted PCR: amplification of an individual sequence flanked by a highly repetitive element from total human DNA. *Nucleic Acids Res*. 1994; 22:3251-2.

45. Hughes S, Arneson N, Done S, et al. The use of whole genome amplification in the study of human disease. *Prog Biophys Mol Biol*. 2005; 88:173-89.

46. Wang G, Brennan C, Rook M, et al. Balanced-PCR amplification allows unbiased identification of genomic copy changes in minute cell and tissue samples. *Nucleic Acids Res*. 2004; 32:e76.

47. Larsen J, Ottesen AM, Lundsteen C, et al. Optimization of DOP-PCR amplification of DNA for high-resolution comparative genomic hybridization analysis. *Cytometry*. 2001; 44:317-25.

48. Peng DF, Sugihara H, Mukaisho K, et al. Alterations of chromosomal copy number during progression of diffuse-type gastric carcinomas: metaphase- and array-based comparative genomic hybridization analyses of multiple samples from individual tumours. *J Pathol*. 2003; 201:439-50.

49. Grant SF, Steinlicht S, Nentwich U, et al. SNP genotyping on a genome-wide amplified DOP-PCR template. *Nucleic Acids Res*. 2002; 30:e125.

50. Lasko D, Cavenee W, Nordenskjold M. Loss of constitutional heterozygosity in human cancer. *Annu Rev Genet*. 1991; 25:281-314.

51. Innis MA, Gelfand DH, Sninsky JJ, et al. Optimization of PCRs. In: Innis MA ed. *PCR Protocols: A guide to Methods and Applications*. Academic Press, New York, NY, USA. 1990:3-12.
52. Sardelli A. Plateau effect – understanding PCR limitations. *Amplifications*. 1993; 9:1-5.
53. Morrison C, Gannon F. The impact of the PCR plateau phase on quantitative PCR. *Biochim Biophys Acta*. 1994; 1219:493-498.
54. Dennis Lo YM. Introduction to the Polymerase Chain Reaction. In: Dennis Lo YM ed. Methods Mol. Med: Clinical Applications of PCR. Humana Press Inc, Totowa, NJ.
55. Chee M, Yang R, Hubbell E, et al. Accessing genetic information with high-density DNA arrays. *Science*. 1996; 274:610-4.
56. Wang DG, Fan JB, Siao CJ, et al. Large-scale identification, mapping, and genotyping of single-nucleotide polymorphisms in the human genome. *Science*. 1998; 280:1077-82.
57. Cho RJ, Campbell MJ, Winzeler EA, et al. A genome-wide transcriptional analysis of the mitotic cell cycle. *Mol Cell*. 1998; 2:65-73.
58. Lockhart DJ, Dong H, Byrne MC, et al. Expression monitoring by hybridization to high-density oligonucleotide arrays. *Nat Biotechnol*. 1996; 14:1675-80.
59. Wodicka L, Dong H, Mittmann M, et al. Genome-wide expression monitoring in Saccharomyces cerevisiae. *Nat Biotechnol.* 1997; 15:1359-67.
60. Solinas-Toldo S, Lampel S, Stilgenbauer S, et al. Matrix-based comparative genomic hybridization: biochips to screen for genomic imbalances. *Genes Chromosomes Cancer*. 1997; 20:399-407.
61. Pinkel D, Segraves R, Sudar D, et al. High resolution analysis of DNA copy number variation using comparative genomic hybridization to microarrays. *Nat Genet*. 1998; 20:207-11.
62. Pollack JR, Perou CM, Alizadeh AA, et al. Genome-wide analysis of DNA copy-number changes using cDNA microarrays. *Nat Genet*. 1999; 23:41-6.
63. Halata Z, Grim M, Bauman KI. Friedrich Sigmund Merkel and his "Merkel cell", morphology, development, and physiology: review and new results. *Anat Rec A Discov Mol Cell Evol Biol*. 2003; 271:225-39.
64. Mir R, Sciubba JJ, Bhuiya TA, et al. Merkel cell carcinoma arising in the oral mucosa. *Oral Surg Oral Med Oral Pathol*. 1988; 65:71-5.
65. Schmidt-Westhausen A, Reichart PA, Gross UM. Gingival metastasis of merkel cell carcinoma: a case report. *J Oral Pathol Med.* 1996; 25:44-7.
66. Antoniades K, Giannouli T, Kaisaridou D. Merkel cell carcinoma in a patient with Recklinghausen neurofibromatosis. *Int J Oral Maxillofac Surg*. 1998; 27:213-4.
67. Bellome J, Bays DR. Merkel cell carcinoma of the ear: report of a case. *J Oral Maxillofac Surg*. 1998; 56:984-8.
68. Longo F, Califano L, Mangone GM, et al. Neuroendocrine (Merkel cell) carcinoma of the oral mucosa: report of a case with immunohistochemical study and review of the literature. *J Oral Pathol Med*. 1999; 28:88-91.
69. Park GC, Shelton JB Jr, Ow RA, et al. Merkel cell carcinoma of the lower lip: a case report and histopathologic study. *Arch Otolaryngol Head Neck Surg*. 1999; 125:907-11.
70. Bickle K, Glass LF, Messina JL, et al. Merkel cell carcinoma: a clinical, histopathologic, and immunohistochemical review. *Semin Cutan Med Surg*. 2004; 23:46-53.
71. Reichel OA, Mayr D, Issing WJ. Oropharyngeal metastasis of a Merkel cell carcinoma of the skin. *Eur Arch Otorhinolaryngol.* 2003; 260:258-60.
72. Hashimoto K. Fine structure of Merkel cell in human oral mucosa. *J Invest Dermatol*. 1972; 58:381-7.
73. Vigneswaran N, Muller S, Lense E, et al. Merkel cell carcinoma of the labial mucosa. An immunohistochemical and ultrastructural study with a review of the literature on oral Merkel cell carcinomas. *Oral Surg Oral Med Oral Pathol*. 1992; 74:193-200.
74. Koss LG, Spiro RH, Hajdu S. Small cell (oat cell) carcinoma of minor salivary gland origin. *Cancer*. 1972; 30:737-41.
75. Benning TL, Vollmer RT, Crain BJ, et al. Neuroendocrine carcinoma of the oral cavity. *Mod Pathol*. 1990; 3:631-4.
76. Slaughter DP, Southwick HW, Smejkal W. Field cancerization in oral stratified squamous epithelium; clinical implications of multicentric origin. *Cancer*. 1953; 6:963-8.
77. Califano J, van der Riet P, Westra W et al. Genetic progression model for head and neck cancer: implications for field cancerization. *Cancer Res*. 1996; 56:2488-92.
78. Braakhuis BJ, Tabor MP, Leemans CR, et al. Second primary tumours and field cancerization in oral and oropharyngeal cancer: molecular techniques provide new insights and definitions. *Head Neck*. 2002; 24:198-206.
79. Braakhuis BJ, Tabor MP, Kummer JA, et al. A genetic explanation of Slaughter's concept of field cancerization: evidence and clinical implications. *Cancer Res*. 2003; 63:1727-30.
80. Ha PK, Califano JA. The molecular biology of mucosal field cancerization of the head and neck. *Crit Rev Oral Biol Med*. 2003; 14:363-9.

81. Hodgson G, Hager JH, Volik S, et al. Genome scanning with array CGH delineates regional alterations in mouse islet carcinomas. *Nat Genet*. 2001; 29:459-64.

82. Snijders AM, Nowak N, Segraves R, et al. ssembly of microarrays for genome-wide measurement of DNA copy number. *Nat Genet*. 2001; 29:263-4.

83. Cowell JK, Wang YD, Head K, et al. Identification and characterisation of constitutional chromosome abnormalities using arrays of bacterial artificial chromosomes. *Br J Cancer*. 2004; 90:860-5.

84. Harle M, Arens N, Moll I, et al. Comparative genomic hybridization (CGH) discloses chromosomal and subchromosomal copy number changes in Merkel cell carcinomas. *J Cutan Pathol*. 1996; 23:391-7.

85. Van Gele M, Leonard JH, Van Roy N, et al. Frequent allelic loss at 10q23 but low incidence of PTEN mutations in Merkel cell carcinoma. *Int J Cancer*. 2001; 92:409-13.

86. Popp S, Waltering S, Herbst C, et al. UV-B-type mutations and chromosomal imbalances indicate common pathways for the development of Merkel and skin squamous cell carcinomas. *Int J Cancer*. 2002; 99:352-60.

87. Van Gele M, Leonard JH, Van Roy N, et al. Combined karyotyping, CGH and M-FISH analysis allows detailed characterization of unidentified chromosomal rearrangements in Merkel cell carcinoma. *Int J Cancer*. 2002;101:137-45.

88. Siironen P, Louhimo J, Nordling S, et al. Prognostic factors in papillary thyroid cancer: an evaluation of 601 consecutive patients. *Tumour Biol*. 2005; 26:57-64.

89. Gerdes J, Lemke H, Baisch H, et al. Cell cycle analysis of a cell proliferation-associated human nuclear antigen defined by the monoclonal antibody Ki-67. *J Immunol*. 1984; 133:1710-5.

90. Kitamura Y, Shimizu K, Tanaka S, et al. ssociation of allelic loss on 1q, 4p, 7q, 9p, 9q, and 16q with postoperative death in papillary thyroid carcinoma. *Clin Cancer Res*. 2000; 6:1819-25.

91. De Micco C, Zoro P, Garcia S, et al. Thyroid peroxidase immunodetection as a tool to assist diagnosis of thyroid nodules on fine-needle aspiration biopsy. *Eur J Endocrinol*. 1994; 131:474-9.

92. Christensen L, Blichert-Toft M, Brandt M, et al. Thyroperoxidase (TPO) immunostaining of the solitary cold thyroid nodule. *Clin Endocrinol (Oxf)*. 2000; 53:161-9.

93. Wu G, Mambo E, Guo Z, et al. Uncommon mutation, but common amplifications, of the PIK3CA gene in thyroid tumours. *J Clin Endocrinol Metab*. 2005; 90:4688-4693.

94. Suarez HG. Genetic alterations in human epithelial thyroid tumours. *Clin Endocrinol (Oxf)*. 1998; 48:531-46.

95. Garcia-Rostan G, Zhao H, Camp RL, et al. ras mutations are associated with aggressive tumour phenotypes and poor prognosis in thyroid cancer. *J Clin Oncol*. 2003; 21:3226-35.

96. Santoro M, Carlomagno F, Hay ID, et al. Ret oncogene activation in human thyroid neoplasms is restricted to the papillary cancer subtype. *J Clin Invest*. 1992; 89:1517-22.

97. Nikiforov YE. RET/PTC rearragement in thyroid tumours. *Endocr Pathol* 2002; 13:3-16.

98. Santoro M, Papotti M, Chiappetta G, et al. RET activation and clinicopathologic features in poorly differentiated thyroid tumours. *J Clin Endocrinol Metab*. 2002; 87:370-9.

99. Fagin JA. Challenging dogma in thyroid cancer molecular genetics-role of RET/PTC and BRAF in tumour initiation. *J Clin Endocrinol Metab* 2004; 89:4264-4266.

100. Tallini G, Santoro M, Helie M, et al. RET/PTC oncogene activation defines a subset of papillary thyroid carcinomas lacking evidence of progression to poorly differentiated or undifferentiated tumour phenotypes. *Clin Cancer Res*. 1998; 4:287-94.

101. Sugg SL, Ezzat S, Rosen IB, et al. istinct multiple RET/PTC gene rearrangements in multifocal papillary thyroid neoplasia. *J Clin Endocrinol Metab*. 1998; 83:4116-22.

102. Collins BJ, Chiappetta G, Schneider AB, et al. RET expression in papillary thyroid cancer from patients irradiated in childhood for benign conditions. *J Clin Endocrinol Metab*. 2002; 87:3941-6.

103. Bongarzone I, Vigneri P, Mariani L, et al. RET/NTRK1 rearrangements in thyroid gland tumours of the papillary carcinoma family: correlation with clinicopathological features. *Clin Cancer Res*. 1998; 4:223-8.

104. Xu X, Quiros RM, Gattuso P, et al. High prevalence of BRAF gene mutation in papillary thyroid carcinomas and thyroid tumour cell lines. *Cancer Res*. 2003; 63:4561-7.

105. Puxeddu E, Moretti S, Elisei R, et al. BRAF(V599E) mutation is the leading genetic event in adult sporadic papillary thyroid carcinomas. *J Clin Endocrinol Metab*. 2004; 89:2414-20.

106. Ciampi R, Knauf JA, Kerler R, et al. Oncogenic AKAP9-BRAF fusion is a novel mechanism of MAPK pathway activation in thyroid cancer. *J Clin Invest*. 2005; 115:94-101.

107. Fusco A, Viglietto G, Santoro M. A new mechanism of BRAF activation in human thyroid papillary carcinomas. *J Clin Invest*. 2005;115:20-3.

108. Vasko V, Hu S, Wu G, et al. High prevelance and possible de novo formation of BRAF mutation in metastasized papillary thyroid cancer in lymph nodes. *J Clin Endocrinol Metab*. 2005; 90:5265-5269.

109. Melillo RM, Castellone MD, Guarino V, et al. The RET/PTC-RAS-BRAF linear signaling cascade mediates the motile and mitogenic phenotipe of thyroid cancer cells. *J Clin Invest*. 2005; 115:1068-1081.

110. Xing M. BRAF mutation in thyroid cancer. *Endocr Relat Cancer*. 2005; 12:245-62.

111. Quiros RM, Ding HG, Gattuso P, et al. Evidence that one subset of anaplastic thyroid carcinomas are derived from papillary carcinomas due to BRAF and p53 mutations. *Cancer*. 2005; 103:2261-8.

112. Elisei R, Romei C, Vorontsova T, et al. RET/PTC rearrangements in thyroid nodules: studies in irradiated and not irradiated, malignant and benign thyroid lesions in children and adults. *J Clin Endocrinol Metab*. 2001; 86:3211-6.

113. Fusco A, Chiappetta G, Hui P, et al. Assessment of RET/PTC oncogene activation and clonality in thyroid nodules with incomplete morphological evidence of papillary carcinoma: a search for the early precursors of papillary cancer. *Am J Pathol*. 2002; 160:2157-67.

114. Bongarzone I, Vigneri P, Mariani L, et al. RET/NTRK1 rearrangements in thyroid gland tumours of the papillary carcinoma family: correlation with clinicopathological features. *Clin Cancer Res*. 1998; 4:223-8.

115. Musholt TJ, Musholt PB, Khaladj N, et al. Prognostic signifi cance of RET and NTRK1 rearrangements in sporadic papillary thyroid carcinoma. *Surgery*. 2000; 128:984-93.

116. Donghi R, Longoni A, Pilotti S, et al. Gene p53 mutations are restricted to poorly differentiated and undifferentiated carcinomas of the thyroid gland. *J Clin Invest*. 1993; 91:1753-60.

117. Fagin JA, Matsuo K, Karmakar A, et al. High prevalence of mutations of the p53 gene in poorly differentiated human thyroid carcinomas. *J Clin Invest*. 1993; 91:179-84.

118. Ito T, Seyama T, Mizuno T, et al. Unique assotiation of p 53 mutations with undifferentiated but not with differentiated carcinomas of the thyroid gland. *Cancer Research*. 1992; 52:1369-1371.

119. Dobashi Y, Sakamoto A, Sugimura H, et al. Overexpression of p53 as a possible prognostic factor in human thyroid carcinoma. *Am J Surg Pathol*. 1993; 17:375-81.

120. Halaban R, Kwon BS, Ghosh S, et al. bFGF as an autocrine growth factor for human melanomas. *Oncogene Res*. 1988; 3:177-86.

121. Meier F, Nesbit M, Hsu MY, et al. Human melanoma progression in skin reconstructs: biological significance of bFGF. *Am J Pathol*. 2000; 156:193-200.

122. Varner JA, Cheresh DA. Integrins and cancer. *Curr Opin Cell Biol*. 1996; 8:724-30.

123. Brooks PC, Montgomery AM, Rosenfeld M, et al. Integrin alpha v beta 3 antagonists promote tumour regression by inducing apoptosis of angiogenic blood vessels. *Cell*. 1994; 79:1157-64.

124. Brooks PC, Stromblad S, Klemke R, et al. Antiintegrin alpha v beta 3 blocks human breast cancer growth and angiogenesis in human skin. *J Clin Invest*. 1995; 96:1815-22.

125. Hynes RO. Integrins: bidirectional, allosteric signaling machines. *Cell*. 2002; 110:673-87.

126. Piotrowicz RS, Orchekowski RP, Nugent DJ, et al. Glycoprotein Ic-IIa functions as an activation-independent fibronectin receptor on human platelets. *J Cell Biol*. 1988; 106:1359-64.

127. Ill CR, Engvall E, Ruoslahti E. Adhesion of platelets to laminin in the absence of activation. *J Cell Biol*. 1984; 99:2140-5.

128. Sonnenberg A, Modderman PW, Hogervorst F. Laminin receptor on platelets is the integrin VLA-6. *Nature*. 1988; 336:487-9.

129. Staatz WD, Rajpara SM, Wayner EA, et al. The membrane glycoprotein Ia-IIa (VLA-2) complex mediates the Mg++-dependent adhesion of platelets to collagen. *J Cell Biol*. 1989; 108:1917-24.

130. Bennett JS, Chan C, Vilaire G, et al. gonist-activated alphavbeta3 on platelets and lymphocytes binds to the matrix protein osteopontin. *J Biol Chem*. 1997; 272:8137-40.

131. Paul BZ, Vilaire G, Kunapuli SP, et al. Concurrent signaling from Galphaq- and Galphai-coupled pathways is essential for agonist-induced alphavbeta3 activation on human platelets.

132. Duperray A, Berthier R, Chagnon E, et al. Biosynthesis and processing of platelet GPIIb-IIIa in human megakaryocytes. *J Cell Biol*. 1987; 104:1665-73.

133. Kolodziej MA, Vilaire G, Gonder D, et al. Study of the endoproteolytic cleavage of platelet glycoprotein IIb using oligonucleotide-mediated mutagenesis. *J Biol Chem*. 1991; 266:23499-504.

134. Bennett JS. Structural biology of glycoprotein IIb-IIIa. *Trends Cardiovasc. Med.* 1996; 6:31-37.

135. Diaz-Gonzalez F, Forsyth J, Steiner B, et al. Transdominant inhibition of integrin function. *Mol Biol Cell*. 1991; 12:1939-51.

136. Albelda SM, Mette SA, Elder DE, et al. Integrin distribution in malignant melanoma: association of the beta 3 subunit with tumour progression. *Cancer Res*. 1990; 50:6757-64.

137. Hieken TJ, Ronan SG, Farolan M, et al. Molecular prognostic markers in intermediate-thickness cutaneous malignant melanoma. *Cancer*. 1999; 85:375-82.

138. Nierodzik ML, Kajumo F, Karpatkin S. Effect of thrombin treatment of tumour cells on adhesion of tumour cells to platelets in vitro and tumour metastasis in vivo. *Cancer Res*. 1992; 52:3267-72.

139. Chen YQ, Gao X, Timar J, et al. Identification of the alpha IIb beta 3 integrin in murine tumour cells. *J Biol Chem*. 1992; 267:17314-20.

140. Tang DG, Onoda JM, Steinert BW, et al. Phenotypic properties of cultured tumour cells: integrin alpha IIb beta 3 expression, tumour-cell-induced platelet aggregation, and tumour-cell adhesion to endothelium as important parameters of experimental metastasis. *Int J Cancer*. 1993; 54:338-47.

141. Chiang HS, Peng HC, Huang TF. Characterization of integrin expression and regulation on SW-480 human colon adenocarcinoma cells and the effect of rhodostomin on basal and upregulated tumour cell adhesion. *Biochim Biophys Acta*. 1994; 1224:506-16.

142. Trikha M, Timar J, Lundy SK, et al. Human prostate carcinoma cells express functional alphaIIb(beta)3 integrin. *Cancer Res.* 1996; 56:5071-8.

143. Trikha M, Raso E, Cai Y, et al. Role of alphaII(b)beta3 integrin in prostate cancer metastasis. *Prostate.* 1998; 35:185-92.

144. Chen YQ, Trikha M, Gao X, et al. Ectopic expression of platelet integrin alphaIIb beta3 in tumour cells from various species and histological origin. *Int J Cancer*. 1997; 72:642-8.

145. Honn KV, Chen YQ, Timar J, et al. Alpha IIb beta 3 integrin expression and function in subpopulations of murine tumours. *Exp Cell Res*. 1992; 201:23-32.

146. Trikha M, Timar J, Lundy SK, et al. The high affinity alphaIIb beta3 integrin is involved in invasion of human melanoma cells. *Cancer Res*. 1997; 57:2522-8.

147. Trikha M, Timar J, Zacharek A, et al. Role for beta3 integrins in human melanoma growth and survival. *Int J Cancer*. 2002; 101:156-67.

148. Sambrook J, Fritsch EF, Maniatis T, Molecular cloning: A laboratory manual. Cold Spring Harbor Laboratory Press, Cold Spring Harbor, NY. 1989.

149. Pfaffl MW. A new mathematical model for relative quantification in real-time RT-PCR. *Nucleic Acids Res*. 2001; 29:e45.

150. Kitajka K, Puskas LG, Zvara A, et al. The role of n-3 polyunsaturated fatty acids in brain: modulation of rat brain gene expression by dietary n-3 fatty acids. *Proc Natl Acad Sci U S A* 2002; 99:2619–24.

151. Puskas LG, Zvara A, Hackler L Jr, et al. Production of bulk amounts of universal RNA for DNA microarrays. *Biotechniques.* 2002; 33:898-904.

152. Puskas LG, Hackler L Jr, Kovacs G, et al. Recovery of cyanine-dye nucleotide triphosphates. *Anal Biochem*. 2002; 305:279-81.

153. Yang YH, Dudoit S, Luu P, et al. Normalization for cDNA microarray data: a robust composite method addressing single and multiple slide systematic variation. *Nucleic Acids Res*. 2002; 30:e15.

154. Balazs M, Adam Z, Treszl A, et al. Chromosomal imbalances in primary and metastatic melanomas revealed by comparative genomic hybridization. *Cytometry*. 2001; 46:222-32.

155. Larramendy ML, Koljonen V, Bohling T, et al. Recurrent DNA copy number changes revealed by comparative genomic hybridization in primary Merkel cell carcinomas. *Mod Pathol*. 2004; 17:561-7.

156. Lehnerdt KH, Broicher R, Tschubel K, et al. Der interessante Fall Nr.49. *Laryngorhinootologie* 2001; 80:687-689.

157. Tesei F, Farneti G, Cavicchi O, et al. A case of Merkel-cell carcinoma metastatic to the tonsil. *J Laryngol Otol*. 1992; 106:1100-2.

158. Takano T, Hasegawa Y, Miyauchi A, et al. Quantitative analysis of thymosin beta-10 messenger RNA in thyroid carcinomas. *Jpn J Clin Oncol*. 2002; 32:229-32.

159. Onno M, Nakamura T, Mariage-Samson R, et al. Human TRE17 oncogene is generated from a family of homologous polymorphic sequences by single-base changes. *DNA Cell Biol*. 1993; 12:107-18.

160. Martinu L, Masuda-Robens JM, Robertson SE, et al. The TBC (Tre-2/Bub2/Cdc16) domain protein TRE17 regulates plasma membrane-endosomal trafficking through activation of Arf6. *Mol Cell Biol.* 2004; 24:9752-62.

161. Chiappetta G, Pentimalli F, Monaco M, et al. Thymosin beta-10 gene expression as a possible tool in diagnosis of thyroid neoplasias. *Oncol Rep.* 2004; 12:239-43.

162. Santelli G, Califano D, Chiappetta G, et al. Thymosin beta-10 gene overexpression is a general event in human carcinogenesis. *Am J Pathol*. 1999; 155:799-804.

163. Hall AK. Thymosin beta-10 accelerates apoptosis. *Cell Mol Biol Res*. 1995; 41:167-80.

164. Califano D, Monaco C, Santelli G, et al. Thymosin beta-10 gene overexpression correlated with the highly malignant neoplastic phenotype of transformed thyroid cells in vivo and in vitro. *Cancer Res.* 1998; 58:823-8.

165. Lee SH, Son MJ, Oh SH, et al. Thymosin {beta}(10) inhibits angiogenesis and tumour growth by interfering with Ras function. *Cancer Res*. 2005; 65:137-48.

166. Diviani D, Abuin L, Cotecchia S, et al. Anchoring of both PKA and 14-3-3 inhibits the Rho-GEF activity of the AKAP-Lbc signaling complex. *EMBO J.* 2004; 23:2811-20.

167. Hanahan D, Folkman J. Patterns and emerging mechanisms of the angiogenic switch during tumourigenesis. *Cell*. 1996; 86:353-64.

168. Semenza GL. Angiogenesis in ischemic and neoplastic disorders. *Annu Rev Med*. 2003; 54:17-28.

169. Maniotis AJ, Folberg R, Hess A, et al. Vascular channel formation by human melanoma cells in vivo and in vitro: vasculogenic mimicry. *Am J Pathol* 1999; 155:739–75.

170. Hendrix MJC, Seftor EA, Hess AR, et al. Molecular plasticity of human melanoma cells. *Oncogene* 2003; 22:3070–5.

171. Hendrix MJC, Seftor EA, Hess AR, et al. Vasculogenic mimicry and tumour-cell plasticity: lesson from melanoma. *Nature Rev Cancer* 2003; 3:411–21.